Aqueous carbonation of EAF steel slag to produce Supplementary Cementitious Material: Effects on mineral composition, hydration reactivity and mechanical properties

Construction and Building Materials 479 (2025) 141361

Contents lists available at ScienceDirect

Construction and Building Materials

journal homepage: www.elsevier.com/locate/conbuildmat

Aqueous carbonation of EAF steel slag to produce Supplementary Cementitious Material: Effects on mineral composition, hydration reactivity and mechanical properties

Francesca Bonfante [a], Giuseppe Ferrara [a,*], Pedro Humbert [b], Davide Garufi [b], Jean Marc Tulliani [a], Paola Palmero [a]

[a] Politecnico di Torino, Department of Applied Science and Technology, INSTM R.U. Lince Laboratory, Corso Duca Degli Abruzzi 24, Torino 10129, Italy
[b] CRH Innovation EMAT, De Klencke 10-12, Amsterdam 1083 HL, the Netherlands

ARTICLE INFO

Keywords:
Carbon capture and utilisation
Electric arc furnace slag
Wet carbonation
Supplementary Cementitious Materials
Carbon footprint

ABSTRACT

This study investigates the reactivity of Electric Arc Furnace (EAF) slag after direct aqueous carbonation, aiming to identify possible mechanisms to qualify it as a Supplementary Cementitious Material (SCM). To this end, pastes and mortars comprising 10, 20 and 30 % of non-carbonated and carbonated EAF slag were prepared. Compressive strength, isothermal calorimetry, bound water and portlandite consumption tests were performed to ascertain whether the EAF slag can be defined as SCM, and to compare its mechanical and hydraulic properties with those of more conventional SCMs. The CO_2 content of the EAF slag after carbonation was 8.6 %. With the R^3 calorimetric test, a certain hydraulic reactivity of the as-received and hydrated EAF slag was detected while only a small residual reactivity for the carbonated slag was evidenced. However, the bound water and the portlandite consumption tests suggested a higher reactivity of the carbonated slag. The compressive strength test after 28 days showed that the mortar replaced with 30 % carbonated EAF slag (EAFC-30) developed higher strength than those replaced with 30 % of as-received (EAFAR-30) or hydrated (EAFHY-30) slag. The compressive strength tests at 3, 7 and 28 days showed a retarded hydration of EAFC-30 compared to EAFAR-30. The slow but significant hardening of the EAFC-30 mortars agreed with the previous tests and compared to the behaviour of the EAFAR-30 samples, indicates that pozzolanic reactions were more prevalent after the carbonation. Finally, a comparative analysis of CO_2 emissions, substitution percentage and strength class was conducted, confirming carbonated EAF slag as a viable solution.

1. Introduction

Cement is the most widely used building material, with production steadily rising to meet the global demand for housing and infrastructure construction [1]. It is estimated that cement production in 2020 was approximately 7 % higher than in 2012 and nearly 50 % higher than in 2003 [2]. As the impacts of global warming become more and more evident, growing attention is focused on cement manufacturing, which account for approximately 5–7 % of anthropogenic CO_2 emissions [3]. To achieve carbon neutrality, the CEMBUREAU 2050 roadmap [4] identified several potential strategies, including clinker substitution and carbon capture and utilisation (CCU). CCU technologies represent a pivotal element within the strategy devised by CEMBUREAU. These technologies are already in existence and consist of capturing the CO_2 from the flue gas through two main mechanisms, namely CO_2 conversion and mineral carbonation. The former aims to produce renewable fuels and chemicals through carbon recycling, while the latter allows for permanent storage of carbon dioxide by forming calcium carbonate. The materials obtained via mineral carbonation may find applications in the construction sector (e.g. bricks, tiles, pavements etc.) [5]. Clinker substitution, instead, is the most effective approach for reducing the carbon dioxide footprint of Portland cement (OPC) and consists of minimizing the clinker content in the final binder [6]. This is achieved through the production of blended or composite cements, whereby supplementary cementitious materials (SCMs) are incorporated at the cement manufacturing facility. According to the CEMBUREAU roadmap to

* Corresponding author.
E-mail addresses: francesca.bonfante@polito.it (F. Bonfante), giuseppe.ferrara@polito.it (G. Ferrara), phumbert@crh.com (P. Humbert), dgarufi@crh.com (D. Garufi), jeanmarc.tulliani@polito.it (J.M. Tulliani), paola.palmero@polito.it (P. Palmero).

https://doi.org/10.1016/j.conbuildmat.2025.141361
Received 24 December 2024; Received in revised form 24 February 2025; Accepted 15 April 2025
Available online 25 April 2025

achieve carbon neutrality in the cement industry by 2050, actions related to clinker substitution, decarbonised raw materials and low-carbon clinker together account for about 15 % of the total CO_2 reduction. Measures related to Carbon Capture Storage and Utilisation account for the largest share, 36 % of the total reduction. The term "supplementary cementitious materials" describe materials that exhibit either hydraulic or pozzolanic behaviour [7]. The majority of SCMs currently in use consists of limestone, ground-granulated blast-furnace slag (GGBS) and coal fly ash. Limestone is available in unlimited quantities and can be substituted up to 35 % [8], however above the 15 % of substitution the cement properties are affected by dilution. On the other hand, GGBS and fly ash together are available in limited amounts, approximately 15 % of total cement production, but could be substituted up to 95 % and 55 % respectively [8]. Furthermore, the availability of both these materials is expected to decline rapidly over the coming years, particularly in Europe [6]. The replacement of coal-fired power plants by cleaner technologies for energy production will reduce the amount of fly ash released [1], while the increasing use of the Electric Arc Furnace (EAF) at the place of the Blast Furnace (BF)/Basic Oxygen Furnace (BOF) integrated technologies will result in a reduction in GGBS production. EAF enables the production of steel from metal scrap, representing a more sustainable steel manufacturing process. Notably, also the steelmaking sector contributes significantly to global CO_2 emissions, accounting for approximately 7 % - 9 % in 2020 [9], and the EAF process is one of the green solutions available. In 2023, the market share of EAF in global steel production accounted for 29 %, with an estimated rise to 40 % in 2030 [10]. Slag production from the EAF process will consequently increase. This process, indeed, generates about 120–170 kg of EAF slag per ton of steel produced [11]. In 2018, the production of EAF steel slag in Europe was documented to be 4 million tons [12], and projections indicate that it will continue to grow in the forthcoming years. However, the utilisation of steel slags remains comparatively low. India and China, which collectively produce approximately 50–55 % of the world's crude steel, landfill more than 70 % of the produced slag [13]. With the further perspective of a transition in the type of slag predominantly produced, it is essential to study methods for re-use of EAF slag, and in particular, to be able to replace the slags generated during more intensive steel processes in their current applications. Steel slags usually exhibit latent hydraulicity, meaning that their hydraulic activity is limited, and the reaction may need to be activated. In addition, while GBBS undergoes rapid cooling (quenching) in order to obtain reactive amorphous phases, EAF slag is typically obtained through a slow cooling process, which results in the formation of crystallised, non-reactive phases.

Consequently, the reuse of EAF slag encountered challenges associated with its low reactivity, inconsistent chemical composition, high water absorption, volumetric instability and possible presence of harmful elements, particularly heavy metals. Recent studies explored various avenues for the treatment and reuse of EAF slag, with a particular focus on its potential applications in asphalt mixtures [11], as a filler in nitrile butadiene rubber [14], as an inert material [15] and aggregates [16]. There has been a notable emphasis on its utilisation in the construction sector, also as SCM [17]. One potential application pertains to the production of clinker-free compact elements through the process of curing in a carbonation chamber characterised by a low water content [18]. Despite the substantial potential in terms of strength, the pre-cast nature of the processed product emerges as a significant limitation, thereby restricting its field of applicability. Furthermore, several studies [19–23] have proposed accelerated direct carbonation of EAF slag as a potential method for simultaneously stabilising the material and obtaining carbon capture and storage. This technique, although showing promising results in terms of carbonation efficiency, raises concerns about the possible reuses of this end-product. Indeed, in an ideal scenario, the EAF slag mineral carbonation would be integrated with the clinker substitution strategy, with the carbonated slag being reused as SCM. This would enable the designation of the process as CCU technology, thereby having a double impact on the Carbon Neutrality by 2050 Roadmap.

Only few studies, some of which are reported thereinafter, have been evaluating the influence of carbonation on the reactivity of steelmaking slags. Fang et al. [24], proposed a wet carbonation of BOF slag for 1, 3, 6, 10 and 30 minutes. The early compressive strength of the mortars containing the carbonated steel slag was observed to increase with respect to the reference mortar containing raw slag. The increase was attributed to the formation of nucleation sites during the accelerated pre-carbonation process. Nevertheless, higher carbonation time resulted in a decline in the compressive strength of the mortar, which was attributed to the consumption of reactive minerals present in the steel slag. A lower reactivity of BOF slag and de-sulphurisation slag as SCM for high carbonation rates was found also by Srivastava et al. [25]. However, the aforementioned study [25] reported a compressive strength that was comparable to that of the cement employed. Conversely, Liu et al. [26] observed the formation of amorphous silica gel after the carbonation of converter slag, which resulted in the acquisition of a pozzolanic reactivity thanks to the carbonation pre-treatment. Finally, a previous study from the authors [27] stated an enhancement of the mechanical properties of EAF slag-based mortars when the slag was previously carbonated. Given the lack of studies concerning the reactivity as SCM of EAF slag after carbonation and the controversial results obtained for different slags at high carbonation degrees, this study proposes to investigate the reactivity of EAF slag after an optimised carbonation process. Fig. 1 represents an overview of the activity carried out on this study. They include three main steps: processing of the powders by hydration and aqueous carbonation; chemical/physical characterisation of the processed powders and comparison with the raw material; analysis of the hydration reactivity. EAF slag was carbonated through direct aqueous carbonation, since the higher liquid-to-solid ratio was found to bring to a more efficient carbonation process, specifically comparing tests performed at medium pressures and temperatures [28]. A previous study by the authors [29] optimised the carbonation conditions, which have been utilised to produce the carbonated EAF slag (Fig. 1). In order to verify the hydration reactivity of EAF slag, mortars and pastes comprising non-carbonated and carbonated EAF slag were evaluated to determine the benefits of accelerating pre-carbonation of this steel slag. Compressive strength test, isothermal calorimetry, bound water and portlandite consumption tests were done to ascertain whether the EAF slag can be defined as a SCM [6], and to compare its mechanical and hydraulic properties with those of more conventional SCMs. Furthermore, the study proposes a literature analysis and comparison between different cement types, specifically CEM I, CEM II and CEM III, and cement containing the carbonated EAF slag. The comparative analysis encompassed not only the attained strength class but also the relative CO_2 emissions.

2. Materials and methods

2.1. Materials characterisation

Electric Arc Furnace (EAF) slag was supplied by CRH Innovation Center for Sustainable Construction. The slag was collected from a French plant and subsequently ground and milled to reach a particle size distribution adequate for the reuse as SCM, and close to that of Portland cement [30]. The particle size distributions of the EAF slag and ordinary Portland cement (OPC) were determined by laser diffraction. The measurements were carried out in dry conditions with a Malvern Mastersizer 3000 AERO S laser granulometer (Malvern Pan'alytical, Worcestershire, UK). The average particle diameter by mass resulted 12.1 μm for OPC and 9.4 μm for the EAF slag (further details in Section 3.1).

The chemical composition of the powdered steel slag and of the Ordinary Portland cement (CEM I 52.5 N) used herein was assessed by means of a Rigaku Supermini 2000 X-ray fluorescence spectrometer (Rigaku, Tokyo, Japan) and it is reported in Table 1. CaO, SiO_2, Fe_2O_3

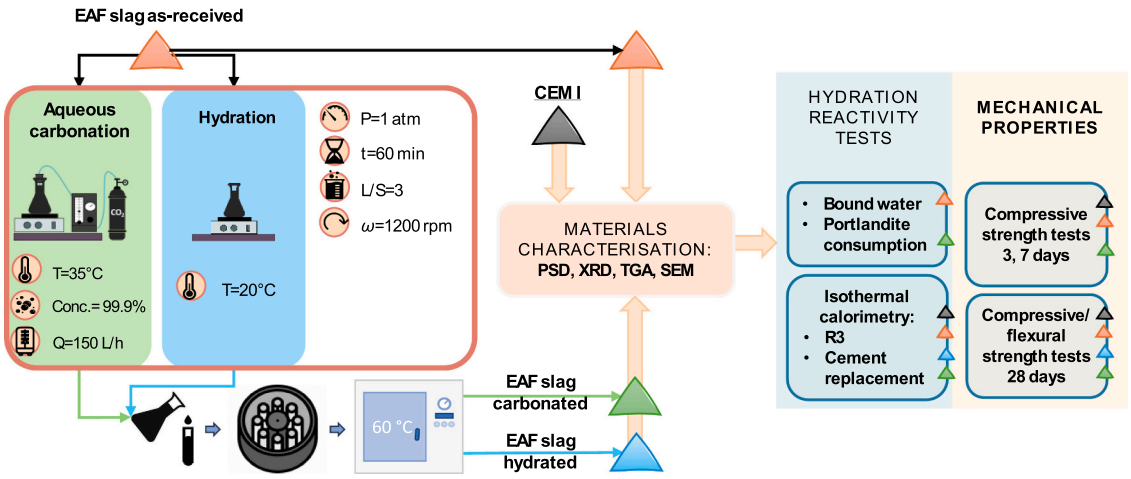

Fig. 1. Overview of the experimental activity.

Table 1
Chemical composition of EAF slag and Ordinary Portland cement (wt%).

	CaO	SiO_2	Fe_2O_3	Al_2O_3	MgO	MnO	V_2O_5	TiO_2	SO_3	LOI
EAF slag	27.1	16.2	30.8	10.5	5.4	4.7	0.1	0.5	0.3	3.1
CEM I 52.5 N	62.2	18.9	2.3	4.3	1.6	0.0	-	0.2	3.8	4.7

and Al_2O_3 are the dominant components of EAF slag, accounting for 27.1, 16.2, 30.8 and 10.5 %, respectively. EAF slag shows a lower content of CaO and SiO_2 with respect to cement, but much higher Fe_2O_3, Al_2O_3, MgO and MnO amounts.

*LOI-Loss on ignition, calculated as the weight loss reached at 1000°C

The crystalline phases were detected using X-ray diffraction (X-ray diffractometer Malvern Panalytical Empyrean, Worcestershire, UK) at 40 kV and 40 mA with a step size of 0.06° and 23 s per step with 2θ spanning from 5–70°, with Bragg-Brentano configuration and a PIXcel detector. Main minerals found in EAF slag (Fig. 2.a) were wuestite (FeO, JCPDF card number 96–900–8637), magnesioferrite (Fe_2MgO_4, JCPDF card number 96–900–3624), akermanite ($Ca_4MgAl_3SiO_{14}$, JCPDF card number 96–900–6115), gehlenite ($Ca_2Al_2SiO_7$, JCPDF card number 96–101–1003), larnite (Ca_2SiO_4, JCPDF card number 96–901–2791), merwinite ($Ca_3MgSi_2O_8$, JCPDF card number 96–900–0286) and iron manganese oxide (Fe_2MnO_4, JCPDF card number 96–230–0619). It was also possible to identify traces of calcium carbonate (JCPDF card number 00–005–0586). The absence of free lime in the raw material was observed, thereby ruling out any potential stability issue related to its use. Meanwhile in Fig. 2.b it is possible to observe the XRD pattern of Ordinary Portland cement, in which it was possible to identify the common cement phases such as tricalcium silicate (alite, C_3S, JCPDF card number 00–049–0442), dicalcium silicate (belite, β-C_2S, JCPDF card number 00–033–0302), brownmillerite or tricalcium aluminate (C_3A, JCPDF card number 00–038–1429), tetra-calcium aluminoferrite (C_4AF, JCPDF card number 00–030–0226) and calcium sulphate (gypsum, $CaSO_4.2H_2O$, JCPDF card number 00–021–0816).

Thermogravimetric/Differential Thermal Analysis (TG-DTA, LABSYS EVO from Setaram, Caluire, France) was used for the qualitative and quantitative assessment of modifications in the material composition. The analyses were conducted at temperatures up to 1050°C at a rate of 10 °C/min in alumina crucibles with nitrogen as the carrier gas at a flow rate of 20 L/min.

The morphology of the particles was characterised using a Phenom XL scanning electron microscope (SEM, Phenom, Ambler, PA, USA), which was equipped with an energy-dispersive X-ray spectroscopy (EDS) detector and operated at an accelerating voltage of 15 kV. Prior to

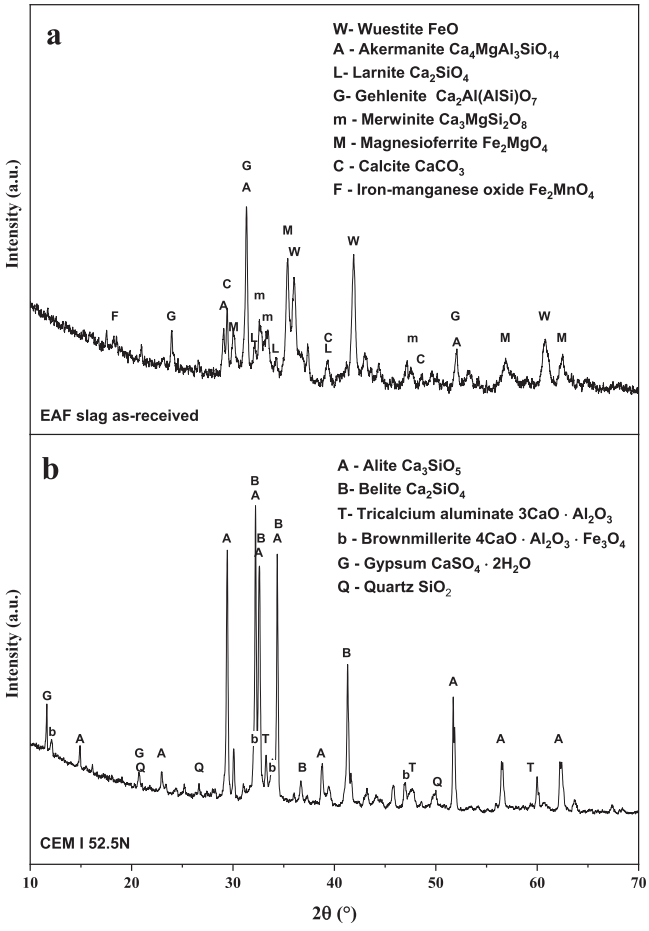

Fig. 2. XRD patterns of a) the EAF slag and b) ordinary Portland cement (CEM I 52.5 N).

SEM characterisation, the as-received and carbonated EAF slag samples were coated with a layer of gold (approximately 30 nm) using SPI Module sputter.

2.2. Experimental design

2.2.1. Accelerated aqueous carbonation

The configuration, already used in Bonfante et al. [31], consists of a 500 mL flask placed on a heating plate and kept under continuous stirring, in order to ensure temperature homogenization. A pipe connects the CO_2 bottle (5.0 grade, SIAD, Italy) to the flask, which is partially closed by a drilled cap maintaining ambient pressure. The direct aqueous carbonation is carried out with a liquid-to-solid ratio of 3, and the flow rate of CO_2 (99.9 vol%) is set at 150 L/h with a flowmeter. A previous study had optimised the reaction time and temperature, which were respectively set to 60 minutes and 35°C, in order to achieve the highest carbonation degree [29]. After the carbonation process, the slurry undergoes a centrifugation step, and the resulting residue is dried in an oven at 60°C for 24 hours. TG-DTA was adopted for the quantification of CO_2. The CO_2 content (m_{CO_2}) is quantified as the difference between the mass of the sample measured at 550°C and 850°C, divided by the mass of the sample before the thermal treatment. Indeed, the weight loss occurring between 550°C and 850°C is commonly associated with the complete decomposition of calcium carbonate and the literature agrees with the use of Eq. 1 for calculating CO_2 uptake [18,32,33]. This equation describes the CO_2 captured by the initial mass of the material (m_i), assuming that the CO_2 captured is the sole contributor to the observed mass gain.

$$\%CO_{2\ \text{uptake}} = \frac{\Delta CO_2}{m_i} \simeq \frac{m_{CO_2\ \text{carbonated}} - m_{CO_2\ \text{initial}}}{1 - m_{CO_2\ \text{initial}}} \quad (1)$$

where $m_{CO2\ carbonated}$ is the content of CO_2 measured in the carbonated sample and $m_{CO2\ initial}$ is the content of CO_2 measured in the as-received sample.

The objective of this study is to investigate the potential for replacing portions of ordinary Portland cement with carbonated EAF slag. The slag was subjected to testing in three distinct phases: as-received (EAFAR), after hydration (EAFHY), and after carbonation (EAFC). The EAFHY was prepared by dispersing the slag in distilled water with a liquid-to-solid ratio of 3 for one hour, followed by centrifuge/drying process with the same procedure used for the carbonated slurry (see Fig. 1). This configuration, consisting of hydration pretreatment without gas injection, was proposed as a means of replicating the EAFC process conditions, except for the CO_2 injection. In this way it was possible to separate the single effect of hydration from the combined effect of hydration and carbonation affecting the slag during the aqueous carbonation.

2.2.2. Hydration reactivity tests

SCMs reactivity testing has become increasingly important especially for non-conventional SCMs which are not well represented by conventional tests developed for cement. Recently, RILEM TC 267-TRM [34] has been developing new reactivity tests for SCMs. In a recent study [35], most of common and novel reactivity tests for SCMs were compared by using compressive strength test on mortars (with 30 % of binder replacement) as a benchmark for the SCMs reactivity. The so-called R^3 test was divided in four possible methodologies: isothermal calorimetry, chemical shrinkage, bound water and portlandite consumption. The tests, at different durations (0.5, 1, 3, 7, 14 days), were compared with compressive strength tests at different curing ages (7, 28, 90 days). The compressive strength test at 28 days, was best predicted by isothermal calorimetry at 7 days (R^2=0.94) and bound water test at 7 days (R^2=0.86), with the other tests with a R^2 below 0.8. Further investigations confirmed the good correlation between these tests and the strength development displayed by SCMs [36], and as an outcome the ASTM C1896 was published [37]. For these reasons, both bound water and calorimetry tests were selected to investigate the reactivity of a non-conventional steel slag and of its carbonated version. R^3-Portlandite consumption test (R^2=0.74), instead, was selected as method for evaluating the pozzolanic reactivity of the materials.

The calorimetry-based testing method assesses the inherent reactivity of the SCM without the influence of cement hydration [38]. In fact, the investigation of SCM/cement blends implies additional challenges, as the hydration of Portland cement and the hydraulic reaction of SCMs occur concurrently, potentially affecting the reactivity of the components in a mutual way [39]. Thus, in the R^3 method, a paste is prepared starting from portlandite, calcite and potassium solution (Table 2), in accordance with the ASTM C1897 [37].

Once clarified the SCMs reactivity, as a following step isothermal calorimetry was carried out on samples produced by blending cement with SCMs, with the aim of investigating the hydration mechanisms that interest mortars with partial replacement of cement with the EAF. The analysis of the heat flow of the two configurations of samples was conducted using an I-Cal 8000 HPC isothermal calorimeter (Calmetrix Inc., Needham, USA), which is equipped with eight channels. The initial tests were conducted following the aforementioned R^3 reactivity test, with the temperature set at 40°C, and the exothermic data collected for 168 hours. The cumulative heat release was calculated according to Eq. 2, in which the cumulative heat is calculated from 75 minutes after the mixing, to allow the sample temperature stabilisation, until the end of the measurement.

$$H_{7d} = \frac{H_{75\text{min}-168h}}{m_{SCM}} \quad (2)$$

where: $H_{75\ min\ -\ 168\ h}$ is the cumulative heat released after the first 75 minutes until 168 hours and m_{SCM} is the mass of EAF slag in the sample analysed.

The second series of tests was conducted on cement pastes with a 30 % partial replacement of cement and a 0.5 water-to-binder ratio (Table 2), in consistency with the parameters used for mortars preparation (see Section 2.2.3). The test was carried out in the same conditions of the R^3 method, i.e. 40°C and 168 hours. Both the tests were conducted on as-received (EAFAR), hydrated (EAFHY) and carbonated (EAFC) slag.

After the hydration of the R^3 pastes for 168 hours, or 7 days, other two reactivity tests were carried out only on EAFAR and EAFC, namely the bound water and the portlandite consumption tests. These tests were performed after drying part of the paste at 40°C for 24 hours [38] in a vacuum oven (Memmert VO29, Büchenbach, Germany) at 5 mbar. Both the tests were carried out using thermogravimetric analysis heating 50 mg of sample from 30°C to 950°C with a ramp of 10 °C/min, in a

Table 2
Details of calorimetry preparation.

ASTM C1897 paste	SCM (g)	Binder (g)		Potassium solution (g)*	$CaCO_3$ (g)
EAFAR	5	$Ca(OH)_2$	15	27	2.5
EAFHY	5	$Ca(OH)_2$	15	27	2.5
EAFC	5	$Ca(OH)_2$	15	27	2.5
Cement paste (30 % replacement)	**SCM (g)**	**Binder (g)**		**Water (g)**	
REF	0	CEM I 52.5 N	40	20	
EAFAR	12	CEM I 52.5 N	28	20	
EAFHY	12	CEM I 52.5 N	28	20	
EAFC	12	CEM I 52.5 N	28	20	

* Potassium solution: for 500 mL of deionized water, 2 g of KOH and 10 g of K_2SO_4.

protective nitrogen atmosphere, obtained with a N_2 flow rate of 20 mL/min. The bound water test was carried out by measuring the water loss at 350°C (Eq. 3), which corresponds to the loss of the water present in the interlayer and to the dehydroxylation of C-S-H.

$$H_2O_{bound} = \frac{\Delta m_{40-350^\circ C}}{m_{dry}} \times 100 \quad (3)$$

where: $\Delta_{m40-350^\circ C}$ is the mass loss in the range 40–350°C and m_{dry} is the initial mass of the dried sample.

The portlandite consumption test verifies the pozzolanicity of a material. A "pozzolan" is defined as a siliceous or siliceous and aluminous material that possesses minimal or no inherent cementitious value but can react with calcium hydroxide exhibiting cementitious properties. For this reason the R^3 portlandite consumption test is conducted on a paste with a known initial quantity of $Ca(OH)_2$. The portlandite consumption is calculated as difference between the initial and the residual content of $Ca(OH)_2$ after 7 days, this value is commonly expressed as portlandite consumed by 100 g of SCM. The residual portlandite content was determined using the tangent method by Lothenbach et al. [40]. The tangent method allows to measure the water loss from portlandite dehydroxylation, therefore it is necessary to convert the mass loss from water to portlandite, through their molar mass, respectively 18 g/mol and 74 g/mol. Eq. 4 shows the passages considering the drying step of the paste.

$$Portlandite\ consumption = \frac{Ca(OH)_{2\ i} \bullet \left(\frac{m_i}{m_{dry}}\right) - \Delta m_{tangent\ method} \bullet \left(\frac{74}{18}\right)}{m_{SCM\ i} \bullet \left(\frac{m_i}{m_{dry}}\right)} \times 100 \quad (4)$$

where: $Ca(OH)_{2i}$ is the mass of portlandite in the sample, m_i is the total mass of the sample prepared, m_{dry} represents the totaol mass of the sample after 24 hours drying in vacuum conditions at 40°C, $\Delta m_{tangent\ method}$ is the mass loss referred to $Ca(OH)_2$, determined by the tangent method, on the sample after 7 days of hydration and 24 hours of drying, and $m_{SCM\ i}$ is the mass of EAF slag in the sample.

2.2.3. Mortars mechanical tests

Compressive strength tests at 28 days of mortars in which the binder was replaced at 30 % have been considered the benchmark for the validation of the R^3 test [35]. The flexural and compressive strengths on mortars were measured by means of the hydraulic press machine (FORM+TEST Prüfsysteme MEGA 100–300–30 DM1, Riedlingen, Germany). The maximum load cell was 30 kN and 300 kN, in force control with a rate of 0.05 kN/s and 1.5 kN/s, for flexural and compression strength apparatus, respectively. The reference mortars were prepared using Portland cement (type I 52.5 N), standard CEN sand and demineralised water. The mortars with EAF slag replacement were prepared with the same Portland cement at a substitution percentage ranging between 10 and 30 wt%. Fresh mixture properties were evaluated through the flow table test by measuring the consistency, expressed in terms of mean diameter d^* of the fresh mortar, obtained after jolting the table 15 times [41]. The mixing, casting and testing processes were conducted in accordance with the specifications outlined in BS EN 196–1 [42]. The specimens were labelled according to the replacement amount and SCM utilised (see Table 3). For each mix proportion, three mortar specimens (40 mm × 40 mm × 160 mm) were prepared to determine the compressive strength of the mortars cured for 3, 7 or 28 days.

$$R_{SCM,\ relative} = \frac{R_{SCM} - R_{PC}}{R_{PC}} \times 100 \quad (5)$$

The relative compressive strength ($R_{SCM,relative}$), calculated according to Eq. 5 as previously proposed by Li et al. [35], was adopted in order to compare the results with previous literature.

where: R_{SCM} and R_{PC} are the absolute strength in MPa of the SCM blended cement and the pure OPC, respectively.

Table 3
Details of mortars preparation.

Mix ID	EAF slag content (% by mass)	Dimensions and number of mortars		
		a × a × h (mm^3)	Number of samples	Curing time (days)
REF	0	40 × 40 × 160	9	3, 7, 28
EAFAR−30	30		9	3, 7, 28
EAFHY−30	30		3	28
EAFC−30	30		9	3, 7, 28
EAFC−20	20		3	28
EAFC−10	10		3	28

REF: reference mortars prepared with OPC; EAFAR- EAF slag as received; EAFHY- EAF slag hydrated; EAFC – EAF slag carbonated.

2.3. CO_2 emissions reduction assessment

The present study proposes an assessment of the impact of EAF slag reuse in cement on its carbon footprint. The blend obtained by partial replacement of carbonated EAF slag is expected to offer a reduction of CO_2 emissions with respect to the cement adopted, combining the strategies of clinker substitution and CCU. The reduction resulting from partial clinker substitution can be determined by applying the percentage of substitution, which signifies the non-use and, consequently, the foregone production of a portion of the cement. The current average CO_2 eq emissions for the cement adopted in this study, a European OPC (CEM I 52.5), were estimated based on five environmental product declarations (see Appendix A), amounting to 791 kg CO_2 eq/ton of cement. The question of whether EAF slag is to be regarded as a waste, with zero CO_2 emissions, or as a by-product is still the subject of debate. In their discussion on this topic, Lizasoain Arteaga et al. [43], concluded that the optimal alternative is to consider as allocated CO_2 emissions only those relative to processes performed exclusively on slags. In any case, EAF technology can reduce the CO_2 emissions by 63–73 % compared to the blast furnace and basic oxygen furnace integrated processes [44], and consequently the associated CO_2 emissions would be reduced as well.

For the aim of this study, it is reasonable to assume the carbon footprint of the EAF slag negligible compared to those related to cement. Given that the implementation from the laboratory scale to a pilot project is still ongoing, also the environmental impacts due to transport, pretreatment and carbonation of EAF slag were not considered. In light of the previous considerations, the CO_2 emissions of cement blends partially replaced by EAF slag were calculated in accordance with Eq. 6. In this equation, R represents the replacement rate, and the CO_2 uptake was recalculated as kg of CO_2 incorporated in the mass of the carbonated slag.

$$CO_{2\ emissions} \cong avgCO_{2emissions\ CEMI\ 52.5}\left[\frac{kgCO_2}{ton\ of\ cement}\right] \times (1-R) - CO_{2\ uptake}\left[\frac{kgCO_2}{ton\ of\ carb.slag}\right] \times R \quad (6)$$

where: $avgCO_{2emissions\ CEM\ I52.5}$ is the average CO_2 eq emissions for the cement type adopted in this study (CEM I 52.5), 791 kg CO_2 eq/ton of cement.

3. Results and discussion

3.1. EAF slag characterisation after the carbonation

The particle size distributions of ordinary Portland cement, as-received, hydrated and carbonated EAF slag, are depicted in Fig. 3.

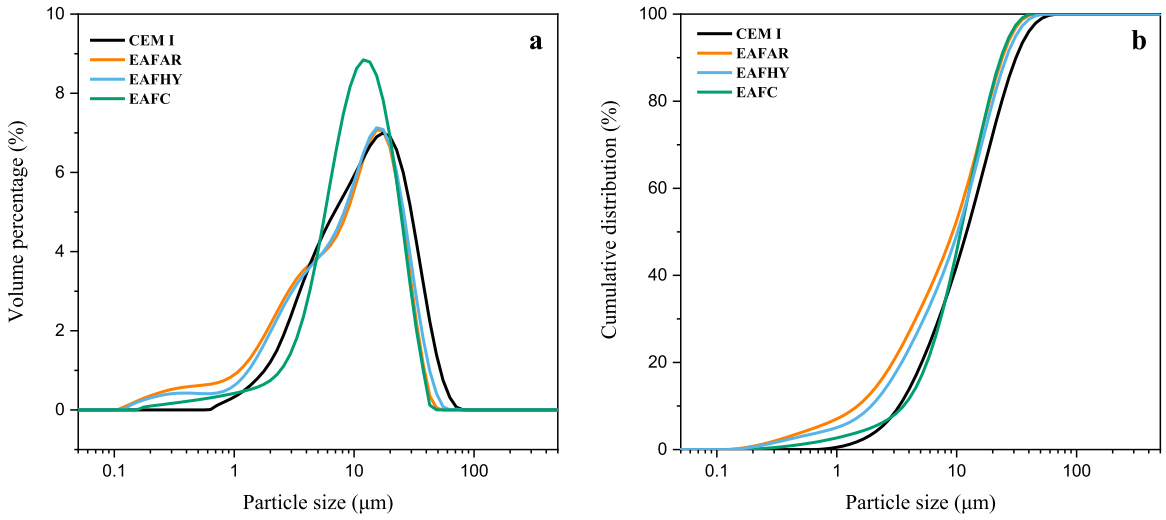

Fig. 3. Frequency (a) and cumulative (b) particle size distribution of cement (CEM I) and EAF slag as received (EAFAR), hydrated (EAFHY) and carbonated (EAFC).

CEM I exhibited a bimodal trend, while EAFAR has a multimodal frequency curve (Fig. 3.a). EAFHY appeared very similar to EAFAR, with pronounced inflection points, while, after the carbonation, the slag showed a monomodal particle size distribution. Overall, the EAF slag resulted in higher fineness than the cement (Fig. 3.b), and specifically the D10, D50 and D90 (the diameter at 10, 50 and 90 % of the cumulative curve distribution) are listed in Table 4. However, the difference in the particle size distribution is minimal and, for the aim of this study, it can be considered negligible. When examining the differences between the slag before and after the carbonation process, it is possible to observe a lower number of particles smaller than 3 μm after carbonation, probably due to the agglomeration of the finest fraction or to the precipitation of calcium carbonate on the surface of the particles. Anyway, D50 and D90 are consistent for the three EAF slag samples.

Fig. 4.a shows the XRD patterns of the as-received, hydrated and carbonated EAF slags. The mineral composition of the as-received material was previously reported (see Fig. 2) and some of the phases (i.e. wuestite, JCPDF card number 96–900–8637), magnesioferrite, JCPDF card number 96–900–3624), akermanite, JCPDF card number 96–900–6115) and gehlenite, JCPDF card number 96–101–1003) did not change during hydration and aqueous carbonation. Most of the changes in the XRD patterns can be observed in the 2θ spans of 27° and 37° (Fig. 4.b). No significant changes in composition were observed after hydration. After carbonation, the peaks associated with calcium carbonate ($CaCO_3$, JCPDF card number 000–005–0586) showed greater intensity, indicating the occurrence of the carbonation reaction. Conversely, peaks associated with larnite (Ca_2SiO_4, JCPDF card number 96–901–2791) and merwinite ($Ca_3MgSi_2O_8$, JCPDF card number 96–900–0286) were undetectable or greatly reduced after carbonation, confirming their involvement in the reactions.

Fig. 5 illustrates the TG-DTA curves of the as-received, hydrated and carbonated EAF slag. The initial content of CO_2 was obtained from the EAFAR curve, resulting in an average of 1.62 % (± 0.22 %). An average CO_2 content of 2.51 % (± 0.11 %) was observed in the hydrated EAF slag, while the CO_2 content after carbonation, 8.63 % (± 0.07 %), exhibited a notable increase. From these data, with Eq. 1, it was possible to calculate the CO_2 uptake of the material, which resulted 7.7 %. The DTA curves highlight a clear shift of the peak relative to calcium carbonate decomposition, and precisely can be observed, which is attributed to the increased stability because of a higher carbonate content [40]. Results align with previous studies from the authors that show a similar increase in calcium carbonate content after the mineralisation process [45,46].

Table 4
Percentile values of the particle size distribution of CEM I, EAFAR, EAFHY and EAFC.

Sample	D10 (μm)	D50 (μm)	D90 (μm)
CEM I	3.31	12.1	31.3
EAFAR	1.51	9.4	24.1
EAFHY	1.94	10.2	26.1
EAFC	3.60	10.8	23.5

Fig. 6 illustrates the scanning electron microscopy (SEM) observations of the EAF slag prior to and following the carbonation process. Prior to the carbonation process (Fig. 6.a), the surface of the particles exhibited a generally smooth surface appearance, characterised by sharp edges. Following the carbonation process (Fig. 6.b), the formation of precipitates on the surface of the particles is evident. In order to gain further insight into the surface chemistry of these particles, an EDS analysis was conducted, where elemental analysis was combined with XRD results (Fig. 4) to identify the compounds involved in the carbonation process. In both figures, a delineated region depicts the EDS map pertaining to the identified elements. Fig. 6.a illustrates the concomitant presence of Ca, Si, and Al, confirming the presence of calcium silicates (larnite) and calcium aluminosilicates (gehlenite and akermanite) in the as-received EAF. Furthermore, the same map reveals the presence of iron-based clusters, specifically wuestite. In Fig. 6.b, the carbonated grain shows calcium as the predominant element of the precipitates. Comparing the two images, it emerges that the different compounds present on the surface of the raw particle are not observed anymore on the carbonated material. Indeed, the surface appears homogeneously covered by calcium compounds of about 1 μm size. Fig. 6 also shows the maps of the intensity of single elements, in particular, oxygen (i), carbon (ii), calcium (iii), iron (iv), aluminium (v) and silicon (vi). From these maps in Fig. 6.a, it is not possible to discern a pattern that would indicate the presence of $CaCO_3$, confirming once again the low initial content of calcite. In contrast, the maps in Fig. 6.b demonstrate a notable correlation between the distribution of carbon and oxygen, which align with the morphology of the precipitates, while calcium is dispersed throughout the surface under investigation. This confirms that during the mineralisation process calcium carbonate precipitates on the external surface of the particles.

3.2. SCMs reactivity tests

3.2.1. R^3 tests

Results from R^3 isothermal calorimetry are shown in Fig. 7 in terms of specific heat rate and cumulative heat release for the as-received,

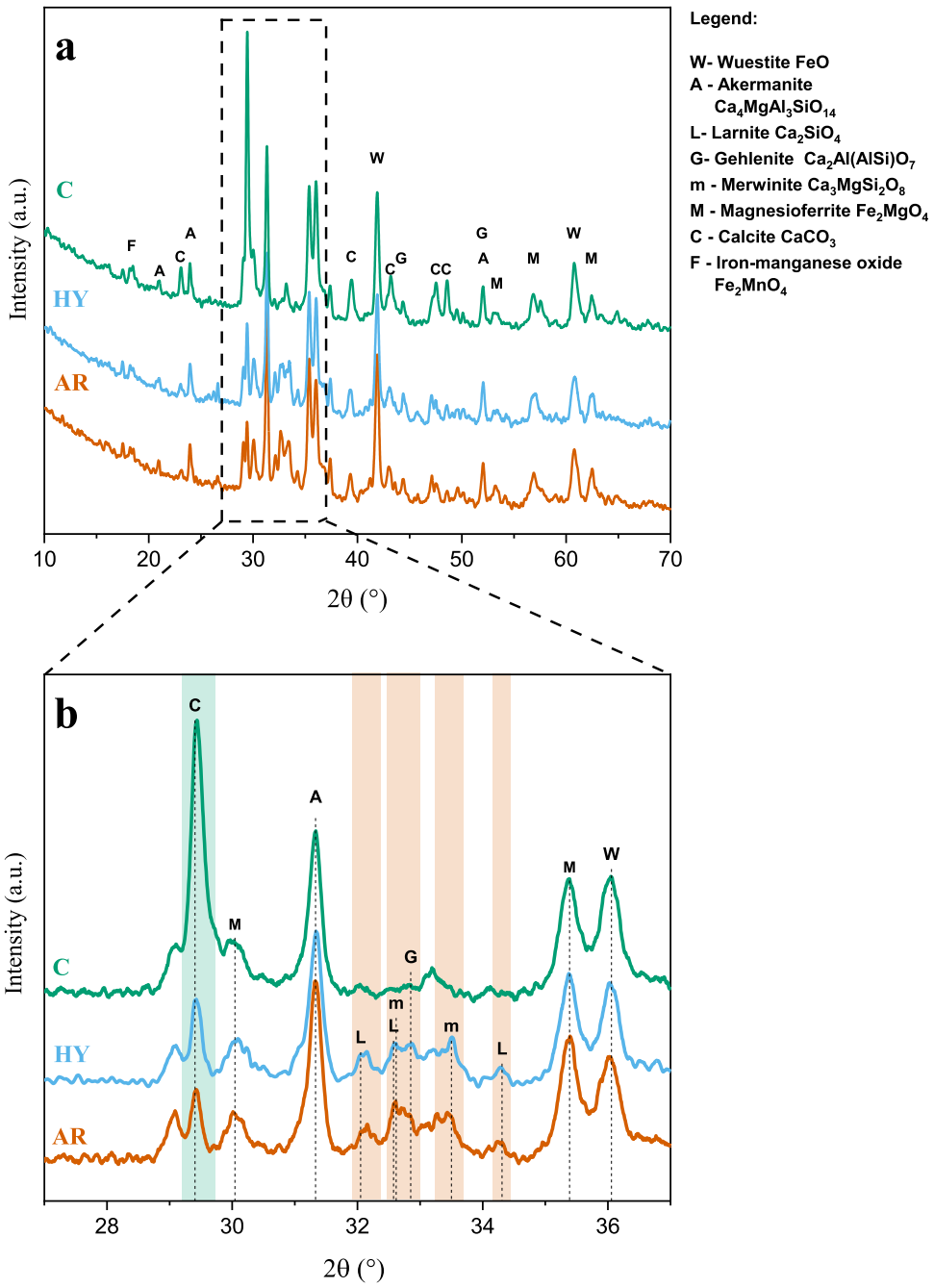

Fig. 4. XRD patterns of EAF slag as received (AR), hydrated (HY) and carbonated (C): **a)** XRD patterns of EAF slag; **b)** Zoom of the XRD patterns in the 27–37 2θ (°) range, to highlight the variation in peaks intensity for calcite (green band) and calcium silicates (orange bands) phases.

hydrated and carbonated EAF slag. In the R^3 isothermal calorimetry-based testing, the temperatures of the samples were stabilised for a period of 75 minutes before the signals were deemed to be accurate. The peaks of the heat flow for EAFAR and EAFHY were reached within these first 75 min (Fig. 7.a), nonetheless they reached higher absolute values than EAFC. The XRD analysis indicated the presence of larnite, a monoclinic polymorph of dicalcium silicate, in both as-received and hydrated slag. As larnite is one of the phases that undergoes carbonation, its presence was not detected anymore in the EAFC samples. The results therefore support the hypothesis, already proposed in literature [47], that the presence of this hydraulic phase contributed to the higher heat flows observed in EAFAR and EAFHY. Fig. 7.b illustrates the specific cumulative heat of the samples. The total cumulative heat at 7 days was found to be 62.5 (± 3.7) J/g of SCM, which is below the threshold (66 % confidence level) of reactivity derived by the TC 267-TRM [36], at 98 J/g of SCM. Therefore, EAFC should be classified as non-reactive. Similarly, EAFAR and EAFHY exhibited a cumulative heat release at 7 days of 91.6 (± 19.6) and 92.0 (± 3.8) J/g of SCM, respectively, which also fell below the threshold. The low reactivity registered is consistent with the process that underwent the EAF slag adopted in this study. In fact, the cooling of EAF slag was achieved in accordance with the conventional methodology, whereby the slag was cooled in a slag heap. This process occurs at a slow rate resulting in the formation of crystalline phases [47] with low or zero reactivity [48]. Considering the observed absence of hydraulic properties following carbonation, together with the residual heat released of EAFC, further investigations regarded its possible pozzolanicity are needed. A previous study on converter slag already identified a residual pozzolanic activity after carbonation [26]

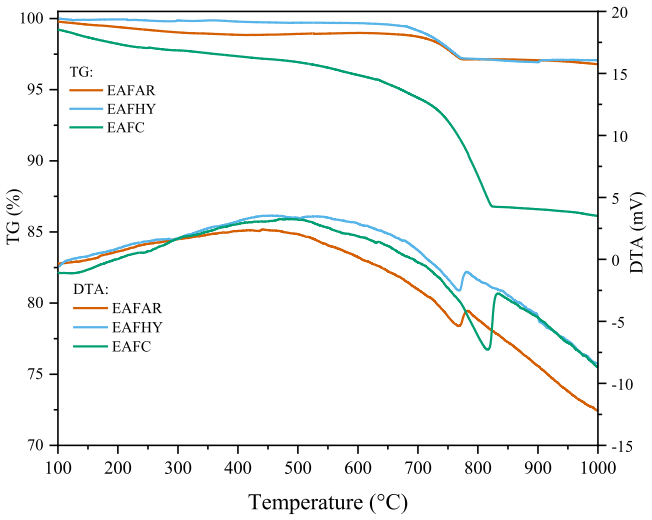

Fig. 5. TGA and DTA curves of EAF slag as received (EAFAR), hydrated (EAFHY) and carbonated (EAFC).

and the reactivity was attributed to the amorphous silica gel formed after the carbonation of the calcium silicates initially detected. In the case of EAFC, only a mild reaction can be discerned.

In order to further investigate the reactivity of the slag after the carbonation, bound water and portlandite consumption tests were carried out on as-received and carbonated (Fig. 8.a-b) EAF slag. The higher reactivity of EAFC with respect to EAFAR in both the tests, confirms that the carbonated material can form a higher quantity of C-S-H by consuming about 50 % more calcium hydroxide with respect to the as-received EAF slag, proving the enhancement of pozzolanic reactivity thanks to the carbonation treatment. The plausible explanation for this phenomenon is that the carbonation of dicalcium silicates in the EAFC not only results in the formation of calcite, but also in the generation of amorphous silica gel [49]. This amorphous phase, not detectable by XRD analysis, when hydrated together with portlandite can react to form secondary C-S-H [26,50]. Based on these results, it can be assumed that the lower heat release of the carbonated EAF slag measured by the isothermal calorimetry indicates a decrease in calcium silicates in favour of a higher pozzolanicity of the material [51]. On the ground of this result, EAFC can be properly classified as SCM.

3.2.2. *Cement replacement calorimetry*

This isothermal calorimetry test was conducted to investigate the effects of partial binder substitution with supplementary cementitious materials (SCMs) on the cement paste during the early hydration phases. Fig. 9 illustrates the specific (with respect to the mass of cement) heat release in the first 16 hours and the cumulative heat of the cement pastes for 168 hours. Although the effect of SCMs on the development of

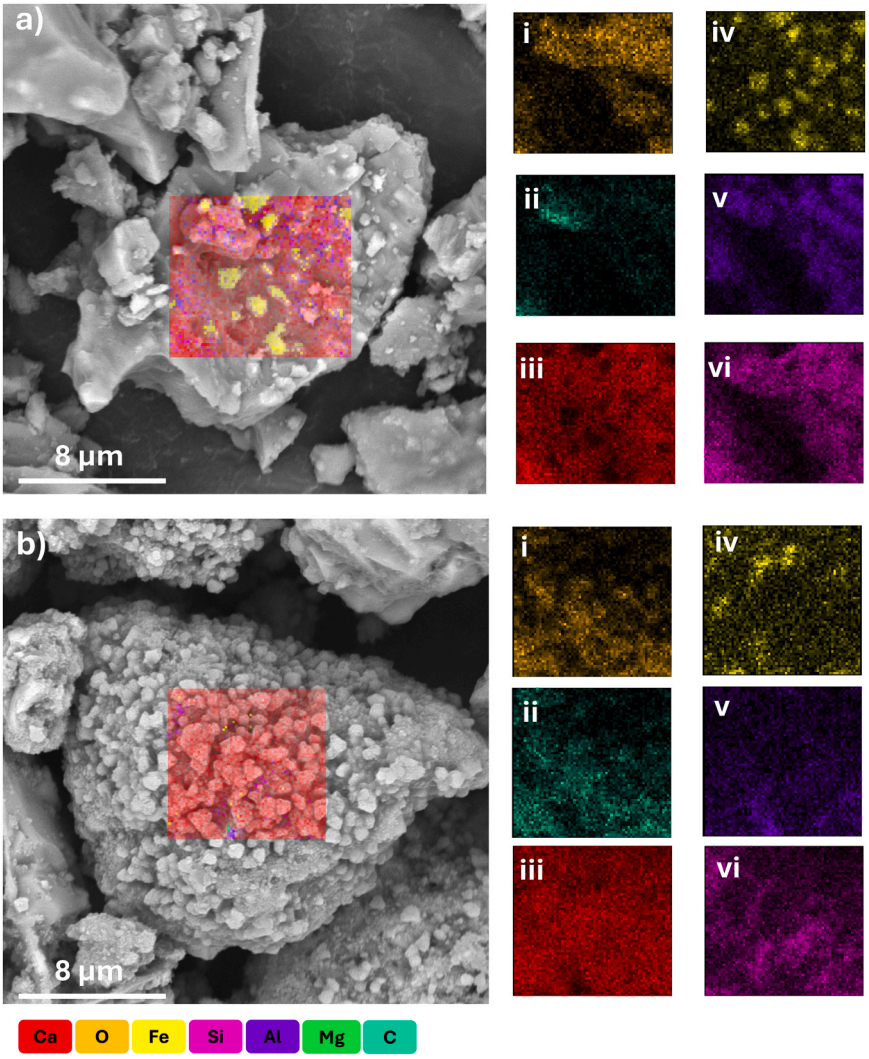

Fig. 6. SEM and EDS element mapping of (a) EAF slag as received and (b) EAF slag carbonated (i. Oxygen, ii. Carbon, iii. Calcium, vi. Iron, v. Aluminium, vi. Silicon).

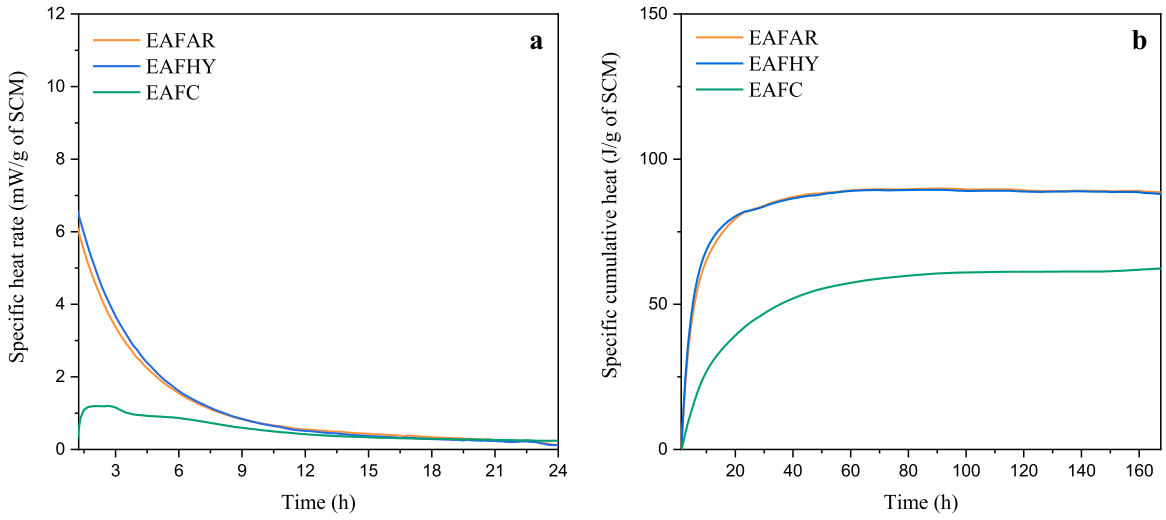

Fig. 7. Specific heat rate (a) and specific cumulative heat (b) by isothermal calorimetry of pastes prepared according to ASTM C1897.

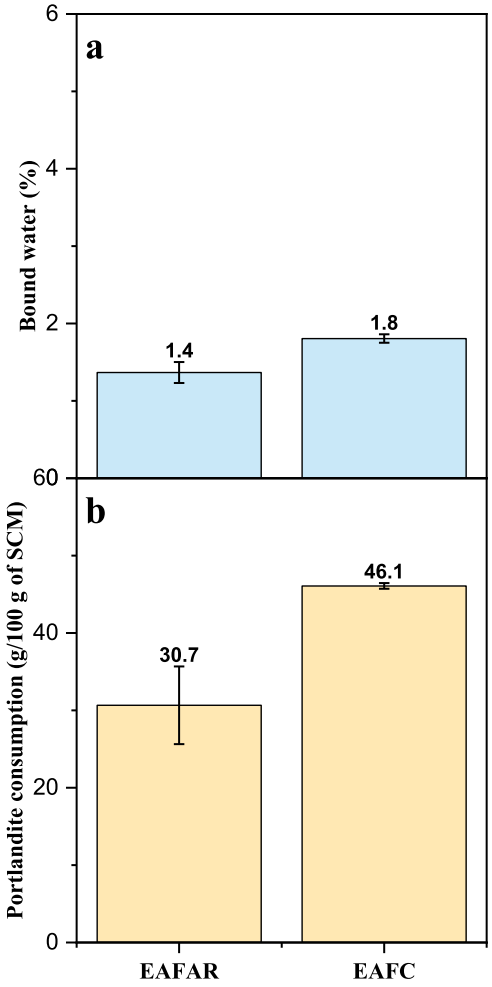

Fig. 8. Bound water (a) and Portlandite consumption (b) of EAF slag as received and carbonated.

strength in blended cement pastes is considered a complex aspect, the reactivity of most SCMs over the first few days is usually negligible [39]. Consequently, the hydration intensity at early ages is mainly influenced by factors such as, water-to-cement ratio (dilution effect), filler effect and nucleation effect, which can be exerted also by inert fillers [52]. Despite normalisation of the heat rate by mass of cement, in Fig. 9.a, none of the blended pastes were able to surpass the initial peak of hydration observed in the reference sample, resulting in a general suppression of the heat rate released. However, the normalised cumulative heat for all the replaced pastes is higher than the reference after the test period of 168 h (Fig. 9.b). This may indicate the occurrence of a filler effect, which, increasing the effective water-to-cement ratio, permits the cement to reach a higher reaction degree, therefore reaching higher final cumulative heat values regardless the lower initial trend.

In Fig. 9.a, it is also possible to observe that the incorporation of EAFAR resulted in a delay in the acceleration phase of the hydration process. The increased water-to-cement ratio can explain the prolonged induction period in the EAFAR-30 [53]. However, this effect does not seem to affect EAFHY-30 and EAFC-30. On the contrary, EAFC-30 showed an earlier onset of the acceleration period. Given that limestone has been observed to exert an accelerating effect on hydration in comparison to other fillers at the same fineness [54], the left shift could be attributed to a more pronounced nucleation effect, obtained after the carbonation thank to the precipitation of calcium carbonate fine particles on the EAF slag surface.

The specific heat rates of EAFAR-30 and EAFHY-30 pastes exhibited a higher second peak in comparison to the reference paste. The second peak is associated with the rapid dissolution of aluminates and has been reported to be more pronounced in Portland cement-slag blends. This effect may be attributed to the slag reaction itself [55–57]. Both EAFAR and EAFHY demonstrate the presence of hydraulic phases, such as larnite, which were absent in the carbonated slag. In fact, EAFC-30 specific heat release, apart from being the lower curve, does not show any additional contribution to the heat release in this phase, with respect to the reference.

Concerning the cumulative specific heat (Fig. 9.b), EAFC-30, the sample comprising carbonated EAF slag, exhibited a superior result, 447 J/g of cement, in comparison to EAFAR-30 and EAFHY-30, which yielded 436 and 444 J/g of cement, respectively. The cumulative heat release of EAFC-30, surpassed the other samples only after 90 hours of the measurement. This late heat release is in line with the pozzolanic reactivity observed on the carbonated sample with the R^3 test.

3.2.3. *Flexural and compressive strength on mortars*

Mortars containing 30 % as-received, hydrated and carbonated EAF slag were prepared and cured for 28 days. The fresh mix properties are shown in Fig. 10. EAFAR increases the workability of the fresh mix (EAFAR-30) compared to hydrated or carbonated slag. Previous studies [26,50] attributed the reduction of workability after the carbonation to an

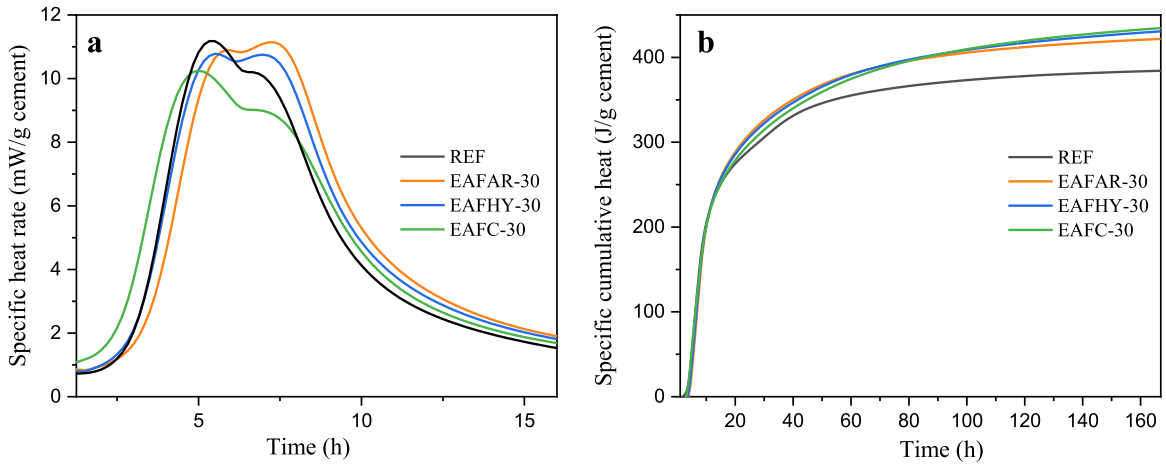

Fig. 9. Specific heat rate (a) and specific cumulative heat (b) by isothermal calorimetry of cement pastes with 30 % partial replacement of SCM.

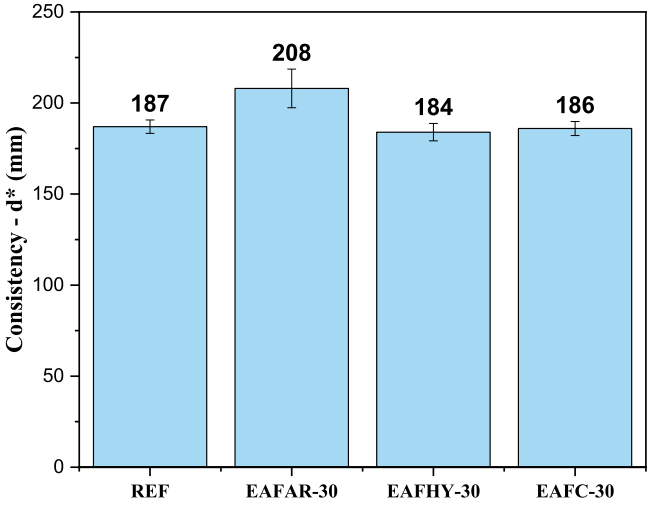

Fig. 10. Consistency of the fresh mortar pastes expressed as average diameter after the flow table test.

increased surface area and pore volume of the carbonated steel slag. The increased surface area is due to the calcium carbonate precipitating on the surface of the slag particles and can result in a higher water demand.

Also mortars with 20 % and 10 % of carbonated slag replacement were prepared and cured for 28 days. The results of the flexural and compressive strength tests are illustrated in Fig. 11. As exhibited in Fig. 11.a, the flexural strength of the mortars exhibited only a marginal reduction of 11.5 % due to the partial substitution, while the impact of slag pretreatment was found to be negligible. All the mortars at 30 % partial replacement exhibited a significative loss of compressive strength with respect to the reference. However, it was observed that the mechanical properties exhibited a slight enhancement when hydrated and carbonated slag were replaced, instead of the as-received material Fig. 11.b). This result is in line with the data of isothermal calorimetry on the cement pastes, which showed a higher cumulative heat released for the carbonated EAF slag.

EAFC-20 showed only a slight enhancement of the mechanical properties, while the substitution at 10 % (EAFC-10) allowed to reproduce compressive strength comparable to the values exhibited by the reference mortars. Fig. 11.c illustrates the relative compressive strength calculated according to Eq. 5. The reference mortar was designated as the baseline and EAFC-30 exhibited a loss of approximately 21 % in compressive strength, showing an improvement with respect to EAFAR-30 (which showed a loss of about 25 %).

Fig. 12 exhibits a focus on the compressive strength development of samples with 30 % partial substitution of cement (EAFAR-30 and EAFC-30 mortars), at 3, 7 and 28 days, compared to the reference mortars. Both replaced samples showed lower early strength in comparison to the reference. Despite that, the compressive strength at three days of EAFAR-30 was significantly higher than that obtained by EAFC-30 (Fig. 12.a). However, at later curing ages EAFC-30 sample gained more strength with respect to EAFAR-30, reaching and overcoming its compressive strength. Even though the samples resulted far from the

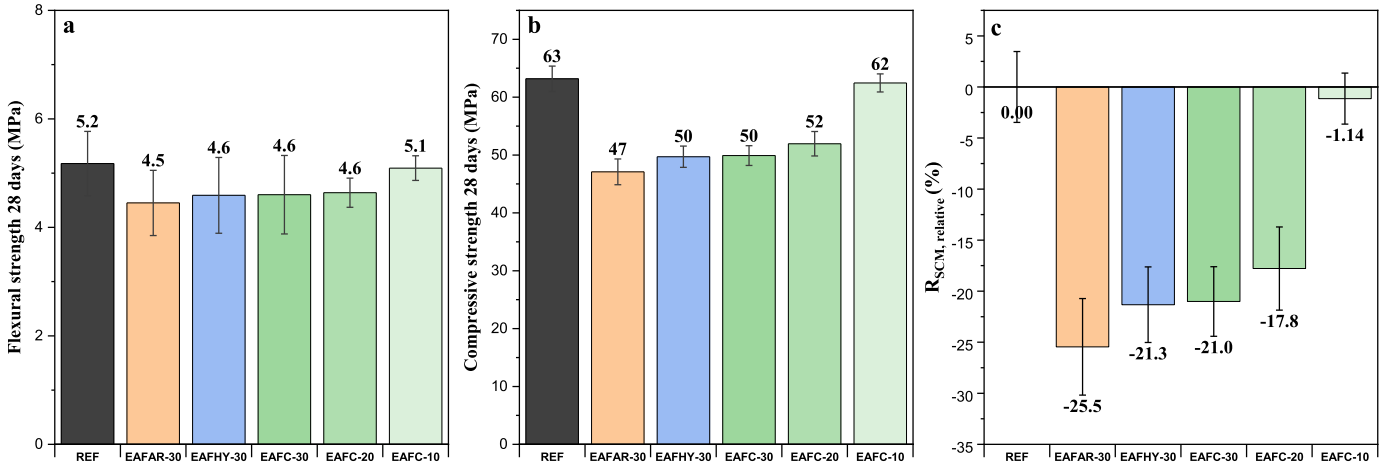

Fig. 11. Flexural strength (a), compressive strength at 28 days (b) and relative compressive strength (c) of mortars containing EAF slag.

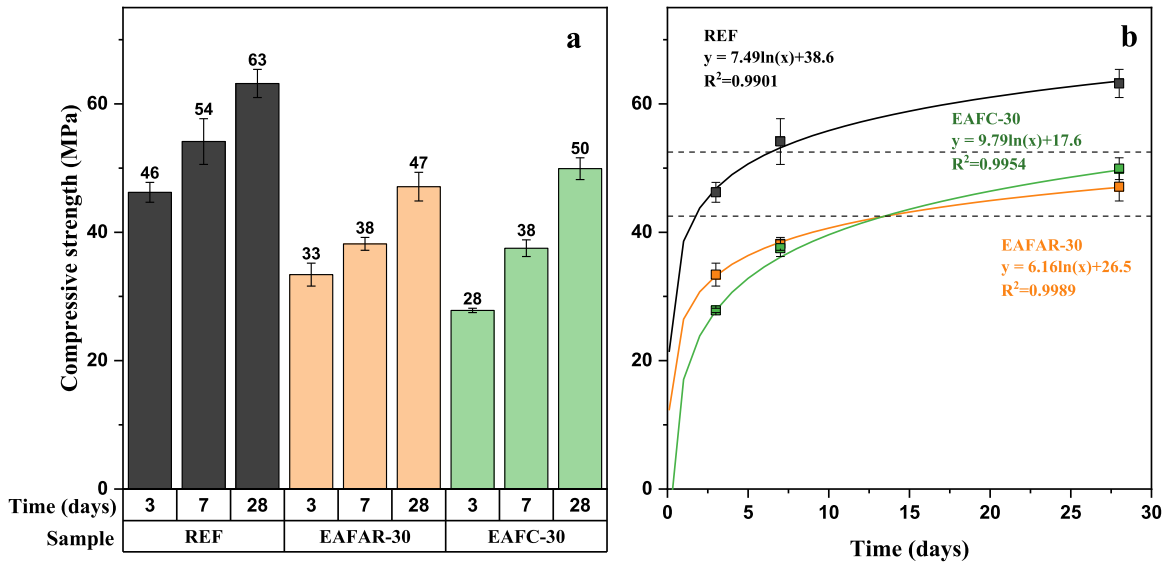

Fig. 12. Compressive strength development of the reference mortar and of the mortars containing EAF slag as received and carbonated, cured for 3, 7 and 28 days.

strength class of the cement adopted as a reference, i.e. 52.5 MPa, their compressive strength was always above the threshold for the strength class 42.5 MPa. The slow, but significant, strength development of EAFC-30 is typically attributed to pozzolanic materials, which have slower reactivity with respect to hydraulic materials. The trend of strength development (Fig. 12.b) is the same trend observed in the calorimetry and confirms the pozzolanic reactivity obtained by the EAF slag after the carbonation.

3.3. Comparison with conventional SCMs

Results from reactivity tests are herein compared with studies from the literature [35,36]. Fig. 13 compares EAF slag reactivity with that of conventional SCMs, specifically from the subgroup composed of slags (SL), pozzolans (PZ) and fly ashes (FA). The y-axis is associated with the 28 days relative compressive strength and the threshold of inert materials is usually associated with the average results from quartz (-35 %). Fig. 13.a presents the correlation between 28-days relative strength and 7-day cumulative heat of conventional SCMs. EAF slag showed a good compatibility with the linear fit obtained by these data. All EAF slag samples positioned around the −25 % and −20 % relative strength, which is within the range individuated for slags. However, the cumulative heat release was similar to that of inert materials. Fig. 13.b shows the relative compressive strength with respect to the bound water at 7 days. From this test, the EAF slag doesn't seem to fit with the conventional SCMs reactivity. However, the misfit could be caused by the different sample preparation and the decision to use a vacuum oven for the drying of the paste. In fact, the drying step, which was necessary for this low-reactive material, performed in a normal oven would have caused the slow conversion of the portlandite into calcite, precluding the possibility to investigate the portlandite consumption. Another factor that may have caused the lower bound water result is to be found in the test methodology. Indeed, the bound water test on the data from literature presented was performed in the muffle at 350°C for 2 hours, while in this study the bound water was quantified from the thermogravimetric analysis. Fig. 13.c depicts the results of the R^3 portlandite consumption test proposed by Li et al. [35]. Due to the low correlation found with the 28-days relative compressive strength, the portlandite consumption was not selected as a novel method for predicting the SCMs reactivity. As a result, only the first tests were carried out and a smaller data set is available. Nevertheless, the test enables the verification of a material's pozzolanic behaviour, which was essential for explaining the improved mechanical performance of the carbonated slag. The EAF slags align with the predicted outcomes, although they did not exhibit high reactivity in comparison with the conventional materials.

3.4. Environmental footprint of carbonated EAF slag-based mortars

Fig. 14 presents a simplified analysis of the environmental advantages of replacing cement with carbonated EAF slag. The figure illustrates the CO_2 emissions in relation to the substitution percentage (Fig. 14.a) and the strength class (Fig. 14.b) of different cement types (i.e. CEM I, CEM II, CEM III), integrated with the findings of this study. The data presented were derived from Environmental Product Declarations of cement produced in Europe and are available for reference in Appendix A. The majority of the selected CEM II and CEM III contain ground-granulated blast furnace slag (GGBS), the most used slag to date.

Regarding the data from the present study, the substitution percentage was known (10 %, 20 % and 30 %), while the CO_2 emissions were calculated from Eq. 6. In order to provide a point of comparison for cement emissions, the average value of emissions for cement production recorded in 1990 (783 kg CO_2/t of cement) was selected as a reference point.

In accordance with the cement types delineated in the UNI EN 197–1 [8], the EAFC-10 and EAFC-20 samples could be classified as a CEM II/A-S, wherein clinker is substituted with 6–20 % by mass of slag, whereas the EAFC-30 sample could be classified as a CEM II/B-S, wherein clinker is substituted with 21–35 % by mass of slag. Fig. 14.a illustrates the correlation between the CO_2 emissions of cements and their clinker substitution ratio. The data demonstrate a linear correlation between CO_2 emissions, and the replacement rate used in the cement, where the highest the rate, the lowest the CO_2 emissions. In Fig. 14.b, there appears to be a direct correlation between the strength development of the samples from this study and the CO_2 emissions. It is noteworthy that the substitution of 10 % (EAFC-10) resulted in a strength development that was comparable to that of the reference mortar, with respective values of 62 and 63 MPa. At the same time, this blend ensures a reduction of around 10 % of the emissions compared to the CEM I 52.5 N adopted, falling within the range of emissions of a CEM II 42.5, while guaranteeing the performances of the higher strength class. In relation to the EAFC-30 and EAFC-20, the compressive strength attained is in accordance with the mean compressive strength specified for cements with a 42.5 strength class. Moreover, the EAFC-30 is situated within the range of CEM II and CEM III CO_2 emissions. Given the compelling need for the cement industry to identify new supplementary cementitious materials due to future scarcity of GGBS and coal fly ash, the carbonated EAF slag poses as a viable option with regard to

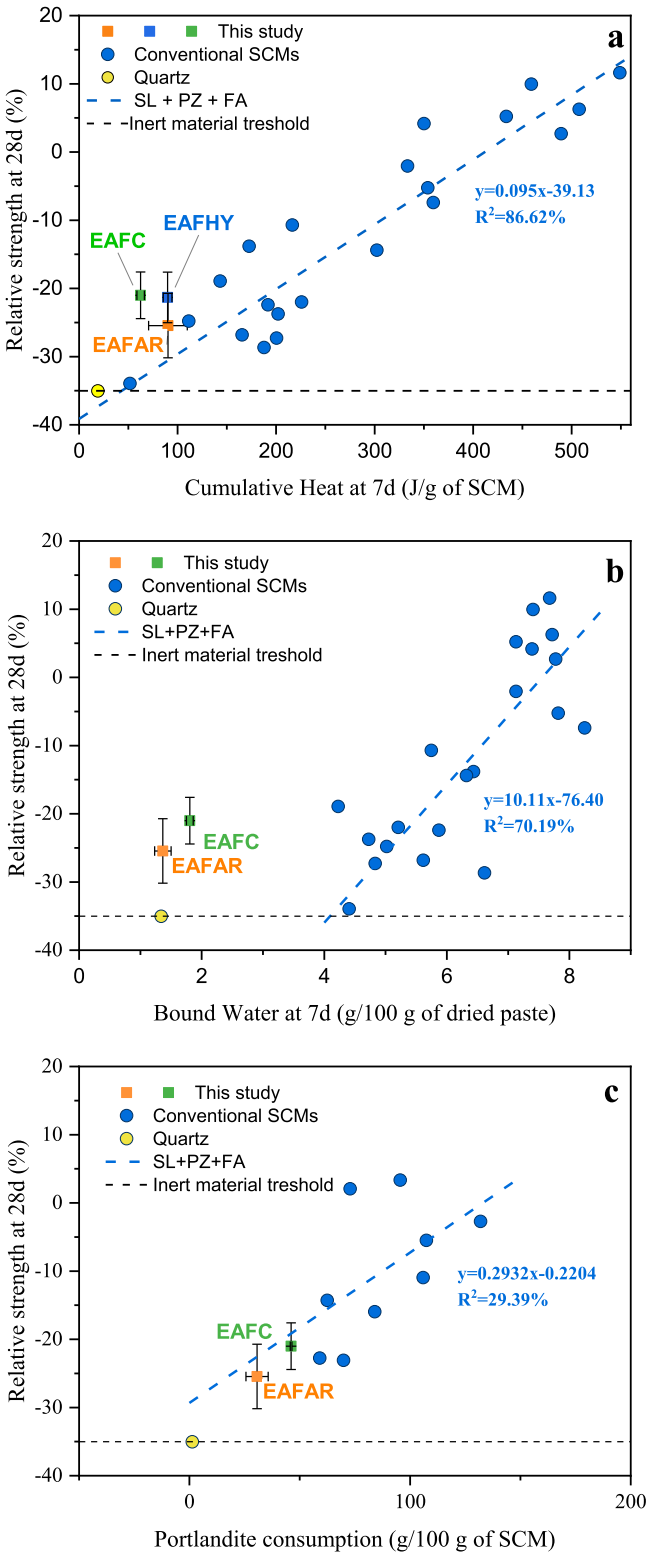

Fig. 13. Linear correlation of R^3 tests – Cumulative heat (a), Bound water (b) and Portlandite consumption (c) – to relative compressive strength at 28 days. Conventional SCMs (data from [35,36]) integrated with results from this study.

environmental impact and performances.

The present evaluation does not take into account the impact of CO_2 emissions resulting from the transportation, pre-treatment, and carbonation process of EAF slag. Nevertheless, it is noteworthy that, in the context of cement, these contributions are likely to be insignificant. In particular, with regard to aqueous carbonation, the optimal integrated process would entail the direct utilisation of flue gas from the clinkerisation process, with a portion of the water undergoing recirculation. Additionally, the high-temperature gases would be used for the drying phase, following a filter press. Furthermore, this process can result more interesting when compared to other processes proposed to increase EAF slag reactivity. Andersson et al. [47], in fact, obtained encouraging outcomes from a remelted and water-granulated EAF slag, while Krammer et al. [58] developed a methodology comprising carbothermal reduction and rapid cooling by wet granulation, coupled with magnetic separation. Such treatments would enhance the performance of EAF slag both for carbonation and for the reuse as SCMs. Indeed, the formation of amorphous phases through rapid cooling, coupled with a reduction in the concentration of metal oxides (including wuestite and magnesioferrite), would result in a markedly more reactive material. However, these high energy impact treatments can become a drawback in terms of sustainable production and are to be balanced with the effective performances that could be obtained by the improved EAF slag.

Finally, despite the potential applications that have already been identified for EAF slag, the possible reuse as SCM would facilitate an upcycling process, thereby enhancing the economic value of this by-product. However, further research is required to progress in this direction. Currently, GGBS is the only component of CEM III recognised within the standard as an 'S' component [8]. To integrate other materials, it is necessary to verify that all the chemicals and durability requirements from the standards are being met. Indeed, EAF slag has an inconsistent chemical composition and may contain harmful elements such as nickel, chromium, cadmium and manganese [59]. Furthermore, aqueous carbonation increases the loss on ignition of the slag, which may ultimately determine a maximum substitution percentage.

A secondary consideration should focus on the cost-effectiveness of the proposed solution. The carbonation process necessitates a comprehensive setup that should be integrated into the existing plant infrastructure. The energy requirements for this process are minimal; however, it is crucial to emphasise the necessity of water treatment, even in scenarios where water recirculation is feasible. Whilst the primary objective of this study is not to evaluate the economic feasibility of the proposed solution, the cost of the substitute clinker and the reduced amount of CO_2 that will be produced should be taken into consideration in order to determine the price of the binder obtained.

4. Conclusions

This study presented a preliminary evaluation of the reactivity of EAF slag after mineral carbonation to test potential applications as SCM. During the carbonation process, the reactive phases such as larnite and merwinite were consumed to form calcium carbonate and the finest fraction of the powder increased in size. The CO_2 content of the EAF slag after mineralisation was 8.6 %. Three stages of EAF slag samples, as-received, hydrated and carbonated, were studied to investigate the reactivity response of the slags to the aqueous carbonation. Isothermal calorimetry, bound water and portlandite consumption tests were conducted on the paste and compared with compressive strength tests on mortars prepared with corresponding binder replacement (30 %). Further mortars with lower binder replacement were tested to study the impact of the carbonated slag. Literature comparison with other non-conventional SCMs and commercially available cements was carried out.

In summary, the main findings can be listed as follows:

- R^3 tests confirmed that even though the as-received slag has some hydraulic reactivity which is lost after the carbonation, a residual reactivity can be observed for the carbonated slag as the portlandite consumption test confirmed an increase in pozzolanic reactivity.
- Results from mechanical compressive tests showed a retarded early hydration development of the carbonated powder with lower strength values at 3 and 7 days compared to the as-received one.

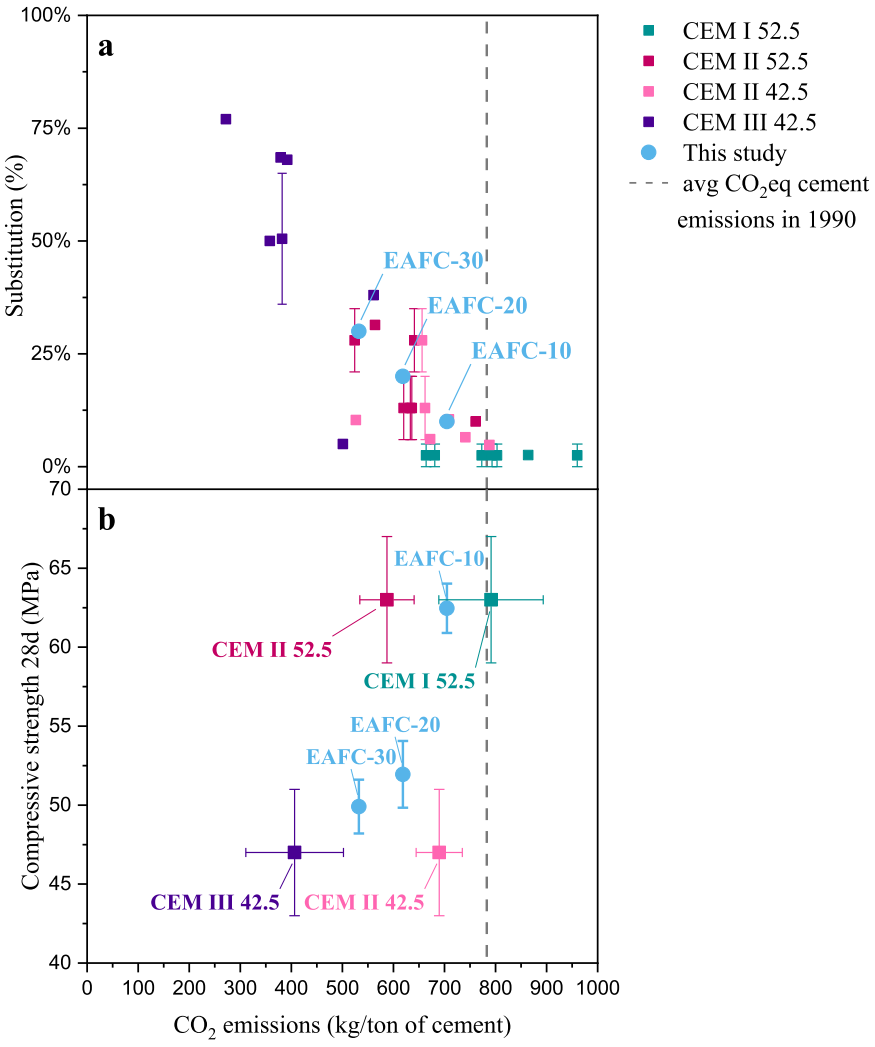

Fig. 14. Overview of CO_2eq emissions of different cement types based on their replacement rate (a), and their compressive strength (b), integrated with the results of this study.

However, a higher compressive strength is shown at 28 days by the mortar containing carbonated slag. This finding indicates that the carbonation process exerts an influence on the hydraulic reactivity of the material, thereby enhancing its pozzolanicity.

- The increased strength development of EAFC-30 with respect to EAFAR-30, can be reconducted to the higher portlandite consumption showed by the carbonated powder. This evidence may be indicative of the formation of a silica gel during the mineralisation process, which subsequently reacted with the portlandite to form secondary C-S-H.
- Comparison with conventional SCMs placed EAF slag in the class of low reactive materials. However, the compressive strength developed was significant. A comparative analysis of CO_2 emissions, substitution percentage and strength class showed a possible fit of the cement-EAFC mix with commercially available cements. In particular, EAFC-30 could fall within the CEM III 42.5 class.

The results of the present work, based on the prospective requirement for novel SCMs and the potential for enhancing the EAF slag characteristics via further pre-treatments, appear promising. However, EAF slag is a feedstock with inconsistent chemical composition, given its origin from steel scrap, and it might be challenging to verify its suitability as SCM according to the harmonised European standards. Furthermore, it is worth to notice that the use of carbonated EAF slag in cement blends to produce mortar may raise concerns related to the long-term durability of the hardened mortar. In this sense, the study paves the way to the investigation of the mechanical properties of the material exposed to moisture and salt attack conditions. Finally, based on the promising results both in terms of mechanical strength and environmental impact, a comprehensive life cycle assessment analysis, considering the integration of the proposed process into clinker- and steelmaking-related industries, is required to provide the correct impact of the mineralisation process on the entire cement production value chain.

CRediT authorship contribution statement

Ferrara Giuseppe: Writing – review & editing, Visualization, Validation, Conceptualization. **Humbert Pedro:** Writing – review & editing, Supervision, Resources, Methodology, Conceptualization. **Garufi Davide:** Writing – review & editing, Supervision, Resources, Data curation, Conceptualization. **Tulliani Jean-Marc:** Writing – review & editing, Validation, Supervision, Conceptualization. **Bonfante Francesca:** Writing – original draft, Visualization, Validation, Methodology, Investigation, Data curation, Conceptualization. **Palmero Paola:** Writing – review & editing, Visualization, Validation, Supervision, Conceptualization.

Declaration of Competing Interest

The authors declare that they have no known competing financial

interests or personal relationships that could have appeared to influence the work reported in this paper.

Acknowledgements

The research described in this paper was financially supported by the European Union's for the PON "Ricerca e Innovazione" 2014–2020 Azione IV.5 - REACT EU projects (DM 1061) and by CRH Innovation Centre for Sustainable Construction Europe. The authors gratefully acknowledge the Safety of Infrastructures and Constructions (SISCON) laboratory for providing the instrumentation for thermal and granulometry analysis.

Conflicts of interest statement

The Authors declare no conflicts of interest.

Appendix A

CEM type	Programme operator	Type of cement	Year	Company	Country	URL	GWP (kg CO_2eq)	Substitution %
CEM I 52.5	DAPconstrucción ®	CEM I 52.5 R	2021	Elite cementos	Spain	https://csostenible.net	773	Other< 5 %
	Bureau Veritas Latvia	CEM I 52.5 R	2020	Schwenk	Latvia	https://schwenk.lv	681	Limestone< 5 % Other < 0.5 %
	The International EPD System	CEM I 52.5 N	2022	Aalborg Portland	Denmark	https://www.aalborgportland.dk	803	Other< 5 %
	EPDItaly	CEM I 52.5 R	2023	HOLCIM	Italy	https://www.epditaly.it	664	Other< 5 %
	EPDItaly	CEM I 52.5 R	2023	Cementirossi	Italy	https://www.epditaly.it	793	Other< 5 %
	EPDItaly	CEM I 52.5 R	2022	Buzzi Unicem	Italy	https://www.epditaly.it	960	Other< 5 %
	EPDItaly	CEM I 52.5 R NOVICEM	2023	Cementi Costantimopoli	Italy	https://www.epditaly.it	864	2.57 %
CEM II 52.5 A o B-S	The Norwegian EPD Foundation	CEM II/A-LL 52.5 N	2022	Schwenk	Latvia	https://www.epd-norge.no	633	Limestone 6–20 % Others < 5 %
	Bureau Veritas Latvia	CEM II A-M (S-LL) 52.5 N	2020	Schwenk	Latvia	https://schwenk.lv	620	Limestone 5–15 % Slag 5–15 % Others < 0.5 %
	The International EPD System	CEM II/A-V 52.5 N	2023	Aalborg Portland	Denmark	https://api.environdec.com	636	Others 0–5 % Fly ash 6–20 %
	Stichting MRPI®	CEM II/B-S 52.5 N	2019	ENCI B.V. Heidelberg Group	Netherlands	https://www.mrpi.nlhttps://www.mrpi.nl/epd-files/epd/1.1.00153.2020%20ENCI_MRPI-EPD.CEM%20II_B-S%2052,5%20N.FINAL.pdf	641	Blast furnace slag 21–35 %
	Stichting MRPI®	CEM II/B-S 52.5 N	2018	Spenner Zement	Germany	https://www.mrpi.nl	564	GGBS 31.4 %
	The International EPD® System	CEM II/A-LL 52.5 R	2023	COLACEM	Italy	https://www.colacem.com	761	Limestone 9.5 % Others 4.8 %
	The Norwegian EPD Foundation	CEM II/B-M (S-LL) 52.5 N	2023	Schwenk	Latvia	https://www.epd-norge.no	524	GGBS 21–35 %
CEM II 42.5 A o B S	The International EPD System	CEM II/A-V 42.5 N	2023	Aalborg Portland	Denmark	https://api.environdec.com	662	Gypsum 0–5 % Fly ash 6–20 %
	EPDItaly	ECOPlanet IIB4 - CEM II/B-LL 42.5 R	2023	HOLCIM	Italy	https://www.epditaly.it	527	10.3 %
	EPDItaly	CEM II/A-LL 45.5 N	2023	Cementirossi	Italy	https://www.epditaly.it	709	10.5 %
	EPDItaly	CEM II/A-LL 42.5 R	2022	Buzzi Unicem	Italy	https://www.epditaly.it	788	4.8 %
	Stichting MRPI®	CEM II/B-M (S-LL) 42.5 R	2018	Dyckerhoff GmbH – Werk Lengerich		https://www.mrpi.nl	656	Slag 21–35 %
	EPDItaly	CEM II A LL 42.5 R ARS (CERTOCEM)	2023	Cementi Costantimopoli	Italy	https://www.epditaly.it	741	Byproducts 6.5 %
	EPDItaly	CEM II B P 42.5 R (TENACEM 42.5 R)	2023	Cementi Costantimopoli	Italy	https://www.epditaly.it	672	Byproducts 6.1 %
CEM III 42.5 A o B	EPDItaly	CEM III A 42.5 N LH-ARS	2023	Cementi Costantimopoli	Italy	https://www.epditaly.it	561	Byproducts 38 %
	The International EPD® System	CEM III/B 42.5 N - LH/SR	2023	COLACEM	Italy	https://www.colacem.com	392	Slag 63.5 % Clinker 32 %
	The International EPD® System	CEM III/B 42.5 N – LH/SR/IAS	2022	COLACEM	Italy	https://www.colacem.com	379	Slag 63.1 % Clinker 31.5 %
	Stichting MRPI®	CEM III/B 42.5	2020	Dyckerhoff GmbH – Werk Neuwied	Germany	https://www.mrpi.nl	272	Slag 77 %
	Stichting MRPI®	CEM III/A 42.5 N / 52.5 L	2019	ENCI B.V. Heidelberg Group	Netherlands	https://www.mrpi.nl	382	BF 36–65 %
	Stichting MRPI®	CEM III A 42.5 N	2021	Ecocem	Ireland	https://www.mrpi.nl	358	Slag 50 %
	Stichting MRPI®	CEM III/A 42.5 N	2019	Phoenix Zementwerke Krogbeumker GmbH & Co. KG	Germany	https://www.mrpi.nl	501	Slag 5 %

Data Availability

Data will be made available on request.

References

[1] K.L. Scrivener, V.M. John, E.M. Gartner, Eco-efficient cements: Potential economically viable solutions for a low-CO2 cement-based materials industry, Cem. Concr. Res 114 (2018) 2–26, https://doi.org/10.1016/J.CEMCONRES.2018.03.015.

[2] K. Wojtacha-Rychter, M. Król, M. Gołaszewska, J. Całus-Moszko, M. Magdziarczyk, A. Smoliński, Dust from chlorine bypass installation as cementitious materials replacement in concrete making, J. Build. Eng. 51 (2022) 104309, https://doi.org/10.1016/J.JOBE.2022.104309.

[3] L. Barcelo, J. Kline, G. Walenta, E. Gartner, Cement and carbon emissions, Mater. Struct. /Mater. Et. Constr. 47 (2014) 1055–1065, https://doi.org/10.1617/S11527-013-0114-5/TABLES/5.

[4] Cembureau, The European cement association - 2019 Activity Report, 2019.

[5] CCU: what is Carbon Capture and Utilisation | CO_2Value Europe, (n.d.). ⟨https://co2value.eu/what-is-ccu/⟩ (accessed January 27, 2025).

[6] F. Zunino, F. Martirena, K. Scrivener, Limestone Calcined Clay Cements (LC3), Mater. J. 118 (2021) 49–60, https://doi.org/10.14359/51730422.

[7] R. Snellings, P. Suraneni, J. Skibsted, Future and emerging supplementary cementitious materials, Cem. Concr. Res 171 (2023) 107199, https://doi.org/10.1016/J.CEMCONRES.2023.107199.

[8] BS EN 197-1:2011 Cement Composition, specifications and conformity criteria for common cements - European Standards, n.d. ⟨https://www.en-standard.eu/bs-en-197-1-2011-cement-composition-specifications-and-conformity-criteria-for-common-cements/⟩ (accessed June 23, 2022).

[9] Climate change and the production of iron and steel - worldsteel.org, (n.d.). ⟨https://worldsteel.org/climate-action/climate-change-and-the-production-of-iron-and-steel/⟩ (accessed February 6, 2025).

[10] Share of EAF route in global steel production likely to rise to 40% in 2030 - BigMint analysis | SEAISI, (n.d.). ⟨https://www.seaisi.org/details/25179?type=news-rooms⟩ (accessed November 27, 2024).

[11] M. Skaf, J.M. Manso, Á. Aragón, J.A. Fuente-Alonso, V. Ortega-López, EAF slag in asphalt mixes: a brief review of its possible re-use, Resour. Conserv Recycl 120 (2017) 176–185, https://doi.org/10.1016/J.RESCONREC.2016.12.009.

[12] EUROSLAG, Statistics 2018, 2018. ⟨https://www.euroslag.com/wp-content/uploads/2022/04/Statistics-2018.pdf⟩ (accessed October 4, 2022).

[13] R. Ragipani, S. Bhattacharya, A.K. Suresh, A review on steel slag valorisation via mineral carbonation, React. Chem. Eng. 6 (2021) 1152–1178, https://doi.org/10.1039/D1RE00035G.

[14] A. Gobetti, G. Cornacchia, G. Ramorino, Reuse of electric arc furnace slag as filler for nitrile butadiene rubber, JOM 74 (2022) 1329–1339, https://doi.org/10.1007/S11837-021-05135-6/FIGURES/8.

[15] A. Primavera, L. Pontoni, D. Mombelli, • Silvia Barella, C. Mapelli, EAF Slag Treatment for Inert Materials' Production, (2015). https://doi.org/10.1007/s40831-015-0028-2.

[16] G. Adegoloye, A.L. Beaucour, S. Ortola, A. Noumowe, Mineralogical composition of EAF slag and stabilised AOD slag aggregates and dimensional stability of slag aggregate concretes, Constr. Build. Mater. 115 (2016) 171–178, https://doi.org/10.1016/J.CONBUILDMAT.2016.04.036.

[17] S.K. Singh, P. Vashistha, R. Chandra, A.K. Rai, Study on leaching of electric arc furnace (EAF) slag for its sustainable applications as construction material, Process Saf. Environ. Prot. 148 (2021) 1315–1326, https://doi.org/10.1016/J.PSEP.2021.01.039.

[18] P.S. Humbert, J.P. Castro-Gomes, H. Savastano, Clinker-free CO2 cured steel slag based binder: Optimal conditions and potential applications, Constr. Build. Mater. 210 (2019) 413–421, https://doi.org/10.1016/J.CONBUILDMAT.2019.03.169.

[19] R. Baciocchi, G. Costa, E. Di Bartolomeo, A. Polettini, R. Pomi, Wet versus slurry carbonation of EAF steel slag, Greenh. Gases: Sci. Technol. 1 (2011) 312–319, https://doi.org/10.1002/ghg.38.

[20] S.O. Omale, T.S.Y. Choong, L.C. Abdullah, S.I. Siajam, M.W. Yip, Utilization of Malaysia EAF slags for effective application in direct aqueous sequestration of carbon dioxide under ambient temperature, Heliyon 5 (2019) e02602, https://doi.org/10.1016/J.HELIYON.2019.E02602.

[21] D. Bonenfant, L. Kharoune, S. Sauvé, R. Hausler, P. Niquette, M. Mimeault, M. Kharoune, CO2 sequestration potential of steel slags at ambient pressure and temperature, Ind. Eng. Chem. Res 47 (2008) 7610–7616, https://doi.org/10.1021/ie701721j.

[22] S.Y. Pan, T.C. Chung, C.C. Ho, C.J. Hou, Y.H. Chen, P.C. Chiang, CO2 mineralization and utilization using steel slag for establishing a waste-to-resource supply chain, 1–11, Sci. Rep. 2017 7 (1) (2017) 7, https://doi.org/10.1038/s41598-017-17648-9.

[23] M.H. Ibrahim, M.H. El-Naas, R. Zevenhoven, S.A. Al-Sobhi, Enhanced CO2 capture through reaction with steel-making dust in high salinity water, Int. J. Greenh. Gas. Control 91 (2019) 102819, https://doi.org/10.1016/J.IJGGC.2019.102819.

[24] Y. Fang, W. Su, Y. Zhang, M. Zhang, X. Ding, Q. Wang, Effect of accelerated precarbonation on hydration activity and volume stability of steel slag as a supplementary cementitious material, J. Therm. Anal. Calor. 147 (2022) 6181–6191, https://doi.org/10.1007/S10973-021-10914-Z/FIGURES/10.

[25] S. Srivastava, M. Cerutti, H. Nguyen, V. Carvelli, P. Kinnunen, M. Illikainen, Carbonated steel slags as supplementary cementitious materials: Reaction kinetics and phase evolution, Cem. Concr. Compos 142 (2023) 105213, https://doi.org/10.1016/J.CEMCONCOMP.2023.105213.

[26] G. Liu, K. Schollbach, P. Li, H.J.H. Brouwers, Valorization of converter steel slag into eco-friendly ultra-high performance concrete by ambient CO2 pre-treatment, Constr. Build. Mater. 280 (2021) 122580, https://doi.org/10.1016/J.CONBUILDMAT.2021.122580.

[27] F. Bonfante, G. Ferrara, P. Humbert, J.M. Tulliani, P. Palmero, CO2 mineralization process of industrial by-products for the production of sustainable mortars, in: 3rd Fib Symposium on Concrete and Concrete Structures, Nov 9th-10th, fib. The International Federation for Structural Concrete, 2023: pp. 355–362.

[28] R. Baciocchi, G. Costa, M. Di Gianfilippo, A. Polettini, R. Pomi, A. Stramazzo, Thin-film versus slurry-phase carbonation of steel slag: CO2 uptake and effects on mineralogy, J. Hazard Mater. 283 (2015) 302–313, https://doi.org/10.1016/j.jhazmat.2014.09.016.

[29] F. Bonfante, G. Ferrara, P. Humbert, D. Garufi, J.M. Tulliani, P. Palmero, Direct aqueous carbonation of Electric Arc Furnace slag: process optimisation through experimental design, Materials and Structures/Materiaux et Constructions (Accepted for Publication) (2025).

[30] R. Snellings, G. Mertens, J. Elsen, Supplementary Cementitious Materials, Rev. Miner. Geochem 74 (2012) 211–278, https://doi.org/10.2138/RMG.2012.74.6.

[31] F. Bonfante, P. Humbert, J.M. Tulliani, P. Palmero, G. Ferrara, CO2 uptake of cement by-pass dust via direct aqueous carbonation: an experimental design for time and temperature optimisation, Mater. Struct. /Mater. Et. Constr. 57 (2024) 1–18, https://doi.org/10.1617/S11527-024-02457-0/TABLES/3.

[32] G. Liu, K. Schollbach, S. van der Laan, P. Tang, M.V.A. Florea, H.J.H. Brouwers, Recycling and utilization of high volume converter steel slag into CO2 activated mortars – The role of slag particle size, Resour. Conserv Recycl 160 (2020) 104883, https://doi.org/10.1016/J.RESCONREC.2020.104883.

[33] M. Mahoutian, Y. Shao, A. Mucci, B. Fournier, Carbonation and hydration behavior of EAF and BOF steel slag binders, Mater. Struct. 48 (2015) 3075–3085, https://doi.org/10.1617/s11527-014-0380-x.

[34] 267-TRM: Tests for reactivity of supplementary cementitious materials, (n.d.). ⟨https://www.rilem.net/groupe/267-trm-tests-for-reactivity-of-supplementary-cementitious-materials-339⟩ (accessed November 22, 2024).

[35] X. Li, R. Snellings, M. Antoni, N.M. Alderete, M. Ben Haha, S. Bishnoi, Ö. Cizer, M. Cyr, K. De Weerdt, Y. Dhandapani, J. Duchesne, J. Haufe, D. Hooton, M. Juenger, S. Kamali-Bernard, S. Kramar, M. Marroccoli, A.M. Joseph, A. Parashar, C. Patapy, J.L. Provis, S. Sabio, M. Santhanam, L. Steger, T. Sui, A. Telesca, A. Vollpracht, F. Vargas, B. Walkley, F. Winnefeld, G. Ye, M. Zajac, S. Zhang, K.L. Scrivener, Reactivity tests for supplementary cementitious materials: RILEM TC 267-TRM phase 1, Mater. Struct. /Mater. Et. Constr. 51 (2018) 1–14, https://doi.org/10.1617/S11527-018-1269-X/TABLES/5.

[36] D. Londono-Zuluaga, A. Gholizadeh-Vayghan, F. Winnefeld, F. Avet, M. Ben Haha, S.A. Bernal, Ö. Cizer, M. Cyr, S. Dolenec, P. Durdzinski, J. Haufe, D. Hooton, S. Kamali-Bernard, X. Li, A.T.M. Marsh, M. Marroccoli, M. Mrak, Y. Muy, C. Patapy, M. Pedersen, S. Sabio, S. Schulze, R. Snellings, A. Telesca, A. Vollpracht, G. Ye, S. Zhang, K.L. Scrivener, Report of RILEM TC 267-TRM phase 3: validation of the R3 reactivity test across a wide range of materials, Mater. Struct. /Mater. Et. Constr. 55 (2022) 1–16, https://doi.org/10.1617/S11527-022-01947-3/FIGURES/10.

[37] ASTM C1897-20 - Standard Test Methods for Measuring the Reactivity of Supplementary Cementitious Materials by Isothermal Calorimetry and Bound Water Measurements - European Standards, (2020). ⟨https://www.en-standard.eu/astm-c1897-20-standard-test-methods-for-measuring-the-reactivity-of-supplementary-cementitious-materials-by-isothermal-calorimetry-and-bound-water-measurements/⟩ (accessed April 16, 2023).

[38] F. Avet, X. Li, M. Ben Haha, S.A. Bernal, S. Bishnoi, Ö. Cizer, M. Cyr, S. Dolenec, P. Durdzinski, J. Haufe, D. Hooton, M.C.G. Juenger, S. Kamali-Bernard, D. Londono-Zuluaga, A.T.M. Marsh, M. Marroccoli, M. Mrak, A. Parashar, C. Patapy, M. Pedersen, J.L. Provis, S. Sabio, S. Schulze, R. Snellings, A. Telesca, M. Thomas, F. Vargas, A. Vollpracht, B. Walkley, F. Winnefeld, G. Ye, S. Zhang, K. Scrivener, Report of RILEM TC 267-TRM phase 2: optimization and testing of the robustness of the R3 reactivity tests for supplementary cementitious materials, Mater. Struct. /Mater. Et. Constr. 55 (2022) 1–14, https://doi.org/10.1617/S11527-022-01928-6/TABLES/6.

[39] B. Lothenbach, K. Scrivener, R.D. Hooton, Supplementary cementitious materials, Cem. Concr. Res 41 (2011) 1244–1256, https://doi.org/10.1016/J.CEMCONRES.2010.12.001.

[40] B. Lothenbach, P. Durdzinski, K. De Weerdt, Thermogravimetric analysis. In: A Practical Guide to Microstructural Analysis of Cementitious Materials, CRC Press, 2018, pp. 196–231. ⟨https://doi.org/10.1201/B19074-5⟩.

[41] EN 1015-3, Methods of Test Mortar for Masonry. Determination of Consistence of Fresh Mortar (By Flow Table), (1999).

[42] BS EN, 196-1 - Methods of testing cement: Determination of strength, British Standards Institution (2016). ⟨https://www.en-standard.eu/bs-en-196-1-2016-methods-of-testing-cement-determination-of-strength/⟩ (accessed March 27, 2024).

[43] E. Lizasoain Arteaga, P. Lastra González, I. Indacoechea Vega, G. Flintsch, Comprehensive analysis of the environmental impact of electric arc furnace steel slag on asphalt mixtures, J. Clean. Prod. 275 (2020) 123121, https://doi.org/10.1016/J.JCLEPRO.2020.123121.

[44] T. Echterhof, Review on the use of alternative carbon sources in EAF steelmaking, Met. (Basel) 11 (2021) 1–16, https://doi.org/10.3390/MET11020222.

[45] F. Bonfante, G. Ferrara, P. Humbert, D. Garufi, J.-M.C. Tulliani, P. Palmero, CO2 sequestration through aqueous carbonation of electric arc furnace slag, J. Adv. Concr. Technol. 22 (2024) 207–218, https://doi.org/10.3151/JACT.22.207.

[46] F. Bonfante, G. Ferrara, P. Humbert, J.M. Tulliani, P. Palmero, Direct aqueous mineralization of industrial waste for the production of carbonated supplementary cementitious materials, RILEM Book. 44 (2023) 581–592, https://doi.org/10.1007/978-3-031-33187-9_54/COVER.
[47] A. Andersson, J. Isaksson, A. Lennartsson, F. Engström, Insights into the valorization of electric arc furnace slags as supplementary cementitious materials, J. Sustain. Metall. 10 (2024) 96–109, https://doi.org/10.1007/S40831-023-00778-Y/FIGURES/12.
[48] E.E. Hekal, S.A. Abo-El-Enein, S.A. El-Korashy, G.M. Megahed, T.M. El-Sayed, Hydration characteristics of Portland cement – Electric arc furnace slag blends, HBRC J. 9 (2013) 118–124, https://doi.org/10.1016/J.HBRCJ.2013.05.006.
[49] W.J.J. Huijgen, R.N.J. Comans, Carbonation of steel slag for CO2 sequestration: leaching of products and reaction mechanisms, Environ. Sci. Technol. 40 (2006) 2790–2796, https://doi.org/10.1021/ES052534B/SUPPL_FILE/ES052534BSI20060223_094507.PDF.
[50] X. Liu, P. Wu, X. Liu, Z. Zhang, X. Ai, The utilization of carbonated steel slag as a supplementary cementitious material in cement, Page 4574 17, Materials 2024 17 (2024) 4574, https://doi.org/10.3390/MA17184574.
[51] P. Suraneni, J. Weiss, Examining the pozzolanicity of supplementary cementitious materials using isothermal calorimetry and thermogravimetric analysis, Cem. Concr. Compos 83 (2017) 273–278, https://doi.org/10.1016/J.CEMCONCOMP.2017.07.009.
[52] P. Lawrence, M. Cyr, E. Ringot, Mineral admixtures in mortars: effect of inert materials on short-term hydration, Cem. Concr. Res 33 (2003) 1939–1947, https://doi.org/10.1016/S0008-8846(03)00183-2.
[53] K.L. Scrivener, P. Juilland, P.J.M. Monteiro, Advances in understanding hydration of Portland cement, Cem. Concr. Res 78 (2015) 38–56, https://doi.org/10.1016/J.CEMCONRES.2015.05.025.
[54] T. Oey, A. Kumar, J.W. Bullard, N. Neithalath, G. Sant, The filler effect: the influence of filler content and surface area on cementitious reaction rates, J. Am. Ceram. Soc. 96 (2013) 1978–1990, https://doi.org/10.1111/JACE.12264.
[55] J.I. Escalante-Garcia, J.H. Sharp, The chemical composition and microstructure of hydration products in blended cements, Cem. Concr. Compos 26 (2004) 967–976, https://doi.org/10.1016/J.CEMCONCOMP.2004.02.036.
[56] C.A. Utton, M. Hayes, J. Hill, N.B. Milestone, J.H. Sharp, Effect of temperatures up to 90°C on the early hydration of portland–blastfurnace slag cements, J. Am. Ceram. Soc. 91 (2008) 948–954, https://doi.org/10.1111/J.1551-2916.2007.02124.X.
[57] X. Wu, D.M. Roy, C.A. Langton, Early stage hydration of slag-cement, Cem. Concr. Res 13 (1983) 277–286, https://doi.org/10.1016/0008-8846(83)90111-4.
[58] A.C. Krammer, K. Doschek-Held, F.R. Steindl, K. Weisser, C. Gatschlhofer, J. Juhart, D. Wohlmuth, C. Sorger, Valorisation of metallurgical residues via carbothermal reduction: a circular economy approach in the cement and iron and steel industry, Waste Manag. Res. (2024), https://doi.org/10.1177/0734242× 241240040.
[59] Y.-J. Wang, J. Tao, J.-G. Li, Y.-N. Zeng, S. Qin, S.-H. Liu, Y.-J.; Wang, M.-J.; Tao, J.-G.; Li, Y.-N.; Zeng, S.; Qin, S.-H. Liu, Carbonation of EAF Stainless Steel Slag and Its Effect on Chromium Leaching Characteristics, (2021). https://doi.org/10.3390/cryst11121498.